Title

Infrasonic tremor wavefield of the Pu`u O`o crater complex and lava tube system, Hawaii, in April 2007

Journal

Journal of Geophysical Research, 115(B12)

ISSN

0148-0227

Authors

Matoza, Robin S
Fee, David
Garcés, Milton A

Publication Date

2010-12-09

DOI

10.1029/2009JB007192

Peer reviewed

Infrasonic tremor wavefield of the Pu`u `Ō`ō crater complex and lava tube system, Hawaii, in April 2007

Robin S. Matoza,[1,2] David Fee,[3,4] and Milton A. Garcés[3]

Received 7 December 2009; revised 12 June 2010; accepted 25 August 2010; published 9 December 2010.

[1] Long-lived effusive volcanism at the Pu`u `Ō`ō crater complex, Kilauea Volcano, Hawaii produces persistent infrasonic tremor that has been recorded almost continuously for months to years. Previous studies showed that this infrasonic tremor wavefield can be recorded at a range of >10 km. However, the low signal power of this tremor relative to ambient noise levels results in significant propagation effects on signal detectability at this range. In April 2007, we supplemented a broadband infrasound array at ~12.5 km from Pu`u `Ō`ō (MENE) with a similar array at ~2.4 km from the source (KIPU). The additional closer-range data enable further evaluation of tropospheric propagation effects and provide higher signal-to-noise ratios for studying volcanic source processes. The infrasonic tremor source appears to consist of at least two separate physical processes. We suggest that bubble cloud oscillation in a roiling magma conduit beneath the crater complex may produce a broadband component of the tremor. Low-frequency sound sourced in a shallow magma conduit may radiate infrasound efficiently into the atmosphere due to the anomalous transparency of the magma-air interface. We further propose that more sharply peaked tones with complex temporal evolution may result from oscillatory interactions of a low-velocity gas jet with solid vent boundaries in a process analogous to the hole tone or whistler nozzle. The infrasonic tremor arrives with a median azimuth of ~67° at KIPU. Additional infrasonic signals and audible sounds originating from the extended lava tube system to the south of the crater complex (median azimuth ~77°) coincided with turbulent degassing activity at a new lava tube skylight. Our observations indicate that acoustic studies may aid in understanding persistent continuous degassing and unsteady flow dynamics at Kilauea Volcano.

Citation: Matoza, R. S., D. Fee, and M. A. Garcés (2010), Infrasonic tremor wavefield of the Pu`u `Ō`ō crater complex and lava tube system, Hawaii, in April 2007, *J. Geophys. Res.*, *115*, B12312, doi:10.1029/2009JB007192.

1. Introduction

[2] The Pu`u `Ō`ō-Kūpaianaha eruption of Kilauea Volcano, Hawaii, has been ongoing since 1983, and activity at Pu`u `Ō`ō between 1992 and 2007 was dominated by persistent effusive eruption, lava tube emplacement, and surface lava flows [*Heliker and Mattox*, 2003]. Although some early volcano acoustic studies provided qualitative descriptions of audible sounds associated with Hawaiian eruptive activity [*Perret*, 1950; *Richards*, 1963], it has only recently been recognized that persistently active Hawaiian eruptions represent near-continuous and energetic sources of low-frequency sound (infrasound, < 20 Hz) [*Garcés et al.*, 2003; *Fee and Garcés*, 2007]. In contrast to the impulsive transient signals characteristic of Strombolian eruptions [*Ripepe et al.*, 2007; *Johnson et al.*, 2008], infrasound radiated by Pu`u `Ō`ō prior to June 2007 consisted of unceasing broadband and harmonic infrasonic tremor, with only minor variation in signal properties over durations of weeks to months. In June 2007 the eruption of Pu`u `Ō`ō paused temporarily before entering a new phase [*Poland et al.*, 2008]. Infrasonic signals associated with this change in eruptive style are not addressed in this study. Here we focus on the continuous tremor source that was characteristic of the eruption prior to June 2007. The first array analysis of the sustained infrasonic tremor wavefield by *Garcés et al.* [2003] revealed a distributed source, consisting of the Pu`u `Ō`ō crater complex and lava tube system flowing along the south flank to the ocean. *Garcés et al.* [2003] postulated that the infrasonic source consisted of the continuous acoustic excitation of a shallow lava-gas mixture beneath the crater area and in horizontal lava tubes, and that this sound could radiate to the atmosphere via vents and skylights. However, the array geometry and instrumental limitations did not allow the accurate localization of infrasound sources to individual vents or regions of the lava flow field.

[1]Institute of Geophysics and Planetary Physics, Scripps Institution of Oceanography, La Jolla, California, USA.
[2]Now at CEA/DAM/DIF, Arpajon, France.
[3]Infrasound Laboratory, University of Hawaii at Manoa, Honolulu, Hawaii, USA.
[4]Now at Wilson Infrasound Observatories, Geophysical Institute, University of Alaska Fairbanks, Fairbanks, Alaska, USA.

0148-0227/10/2009JB007192

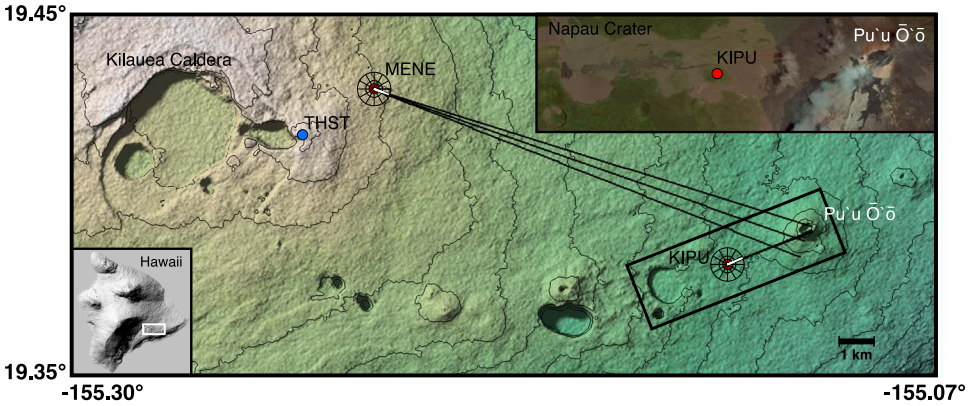

Figure 1. Location of broadband infrasound arrays KIPU and MENE at ~2.4 km and ~12.5 km from Pu`u `Ō`ō, respectively, and Thurston wind tower (THST). Contours at 50 m intervals. Radial histograms of PMCC detection azimuths are shown at array locations, while solid black lines extending from arrays are great circle paths of the median and interquartile range of detection azimuths during the data period Julian day 109–117 2007 UTC (see Figure 2). Box around KIPU and Pu`u `Ō`ō shows area of top right inset. Bottom left inset indicates area of main figure.

[3] Further investigations of this persistent infrasonic tremor wavefield by *Fee and Garcés* [2007] revealed that, at a range of ~12.5 km from Pu`u `Ō`ō, tremor signal power exhibited clear diurnal variations that were anticorrelated with wind speed. Weather balloon data also indicated the formation and breakup of a nocturnal boundary layer for this region, correlated with the diurnal cycle of infrasonic signal reception. These observations indicate the importance of tropospheric (mesoscale and microscale) atmospheric propagation effects on infrasonic signal reception at the ~10 km range. In particular, this range corresponds to the classical acoustic shadow zone predicted by high-frequency ray theory for ordinary diurnal atmospheric conditions, and it was proposed that the presence of a nocturnal boundary layer may act to duct the tremor signal to the array [*Fee and Garcés*, 2007]. However, the accuracy of ray theory begins to fail for the wavelengths and scale lengths considered due to low-frequency effects such as diffraction. For instance, a typical nocturnal boundary layer may extend to ~200–300 m in height above the ground, while the wavelength of a 1 Hz infrasonic signal is ~340 m for a sound speed of ~340 m/s in air. These propagation effects therefore remain incompletely understood.

[4] In order to further investigate the source and regional propagation of Pu`u `Ō`ō's infrasonic tremor wavefield, we conducted a campaign-style field deployment of infrasound and seismic sensors in the vicinity of Pu`u `Ō`ō from 17 to 27 April 2007, and used an infrared camera to help identify candidate infrasonic sources. This paper presents a preliminary investigation of this data set. In addition to characterizing the observed propagation effects, we describe the spectral properties of the continuous infrasonic tremor and discuss potential source processes.

2. Field Deployment

[5] A broadband infrasound array has been operating continuously at MENE (Figure 1) since September 2006 [*Fee et al.*, 2010], and has captured the entire range in Kilauea's eruptive activity from 2006 to present [*Fee et al.*, 2010]. During 17–27 April (Julian day 107–117) 2007, we deployed an additional array, KIPU, ~2.4 km to the southwest of the Pu`u `Ō`ō crater complex, perpendicular to the lava tube system that extends from the crater complex on the south flank (Figure 1). Each array consisted of four Chaparral 2.2 microphones (flat response 0.1–200 Hz). At KIPU, the infrasound sensors were deployed as a centered triangle with ~90 m aperture in a Kipuka (area of surviving land surrounded by lava flows) consisting of densely overgrown ferns within tall trees, providing excellent wind shelter (Figure 1). Initially, one 15 m porous hose was attached to each infrasonic sensor for additional spatial wind filtering. However, heavy rainfall during the first 3–4 days of the experiment resulted in the hoses becoming water-saturated, affecting the system response. Consequently, we removed the hoses (see section 3). A three-component Nanometrics Trillium 40 broadband seismometer (flat response 0.025–50 Hz) was deployed in addition to the infrasound array at KIPU. Data were sampled at 40 Hz with a Reftek 24-bit digitizer. Infrared imaging was performed using an Indigo TVS 700.

3. Propagation of the Tremor Wavefield

[6] The array data were processed using the progressive multichannel correlation (PMCC) algorithm [*Cansi*, 1995], (window length 10 s, time step 1 s, 10 frequency bands between 0.5 and 5 Hz). Figure 2 shows PMCC detection azimuths as a function of time for both MENE and KIPU during the period of KIPU data coverage, color-scaled by the RMS signal power of the detection in dB re 20 μPa. The results are shown underlain by the ambient noise spectrum at the central array element of each array in the 0–1 Hz band, and wind speed at Thurston wind tower (THST, Figure 1). THST is above the forest canopy and the data are therefore likely representative of winds in the study region. *Fee and Garcés* [2007] noted that noise in the 0.02–0.3 Hz band is

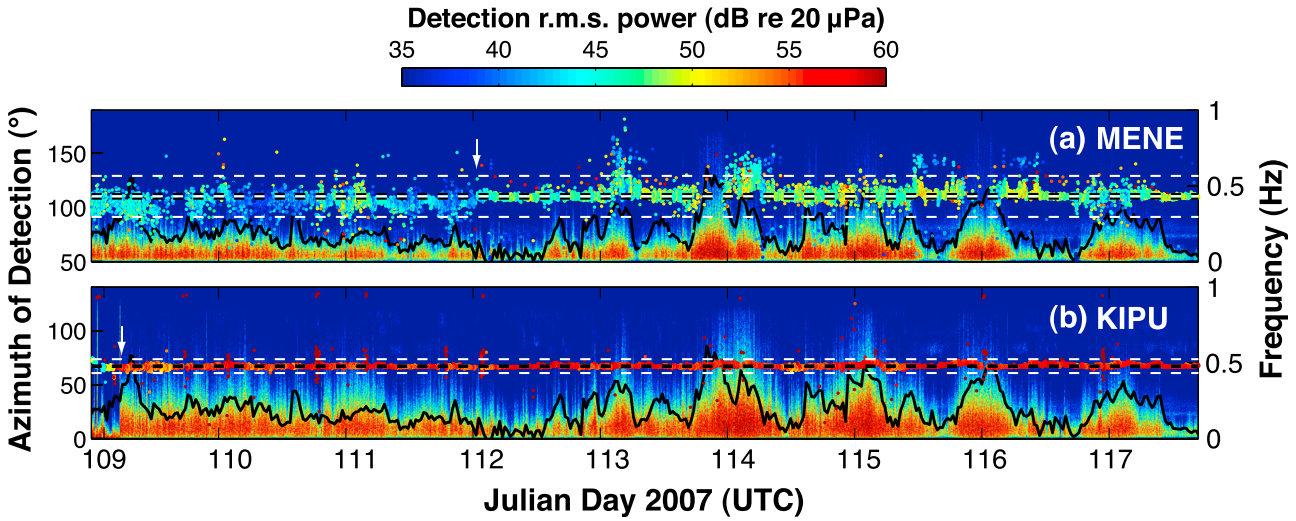

Figure 2. Progressive multichannel correlation (PMCC) array processing results (0.5–5 Hz) superimposed upon low-frequency noise spectrogram (0–1 Hz) of the central array element for each array at (a) MENE and (b) KIPU for the data period Julian day 109–117 2007 UTC. Solid black lines denote wind speed at THST (relative scale, peak value ~9 m/s). PMCC detection azimuths plot as a function of time and color-scaled for RMS power of detected signal in dB re 20 μPa (top color scale). Increases in signal power at KIPU at ~0230 UTC Julian day 109 and at MENE at ~0000 UTC Julian day 112 (white arrows) result from the removal of water-saturated porous hoses from the infrasonic sensors. Horizontal dashed lines are the median (central white), interquartile range (black), and standard deviation from the 10% trimmed mean (outer white) for all detections in the data period (see Figure 1). Noise in the 0.02–0.5 Hz band at each array is well correlated with regional wind speed. KIPU's proximity to the source and downwind direction assure that wind propagation effects on detection azimuth and signal power are minimal. A greater degree of scatter in azimuth values and signal power variation is observed at MENE, well correlated with regional wind speed variations.

well correlated with the regional wind speed. Here we observe that this wind noise extends up to ~0.5 Hz, possibly because the porous hose wind filters were removed, or perhaps simply because different wind noise conditions existed during the time of this experiment than during the data period considered by *Fee and Garcés* [2007] [e.g., *Raspet et al.*, 2006, 2008].

[7] At MENE, azimuthal scatter (azimuthal standard deviation ~18.9°) and variation in signal power (~7–8 dB) is observed for the continuous infrasonic tremor signal originating from Pu`u `Ō`ō during the study period (Figure 2). Occasionally, full loss of coherent signal is observed and is correlated with an increase in regional wind speed (e.g., end of Julian day 113, end of Julian day 115). As described by *Fee and Garcés* [2007], this switching on and off of PMCC detections at MENE is not simply a result of coherent infrasonic signals being overwhelmed by increasing wind noise levels. Overall power spectral levels actually decrease in the bandwidth of the tremor signal (~0.5–3 Hz) during the times in which wind noise in the 0.02–0.5 Hz band increases, indicating that propagation of the tremor signal is somehow inhibited by the change in atmospheric conditions associated with the wind noise increase [*Fee and Garcés*, 2007]. Despite similar atmospheric conditions, scatter in azimuth values and signal power variations are minimal at KIPU. There, an unceasing tremor signal is received from the direction of the Pu`u `Ō`ō crater complex with a smaller azimuthal deviation (azimuthal standard deviation ~6.4°), which may correspond to a distributed source (section 4). Signal power variations ~2–3 dB at KIPU may result from changes in the source signal power in addition to propagation effects.

[8] Two of the signal power changes shown in Figure 2 are the result of equipment changes, and are not the result of real changes in the source power or propagation effects. We removed the porous hoses from KIPU at ~0230 UTC Julian day 109 2007, and from MENE at ~0000 UTC Julian day 112 2007 since they had become saturated by heavy rainfall. In each case, removing the hoses resulted in a ~5 dB increase in observed signal power (Figure 2, white arrows). This large change in the system response is probably a result of the pores in the hoses being filled by water, limiting effective acoustic transmission into the hoses and to the sensor. Such a large change in response is not expected for dry hoses operating under less humid conditions.

[9] We note that the median azimuth for tremor signal at MENE is ~110.4°, ~1–2° higher than the true Pu`u `Ō`ō azimuth of ~108.9° (Figures 1 and 2). This can be partially attributed to deflection of the signal by the prevailing east-northeasterly trade wind as observed at THST for this time period. Assuming a sound speed of ~340 m/s, the time of flight for infrasound from Pu`u `Ō`ō to MENE (12.5 km) is ~37 s. During this time a wind speed of ~9 m/s blowing from the ENE (approximately perpendicular to the propagation path) would deflect the signal ~37 × 9 ~330 m to the SW of the array causing an azimuth deviation of ~$\tan^{-1}$ (330/12500) ~1.5°. This is in good agreement with the observed median azimuthal deviation. A wind speed of

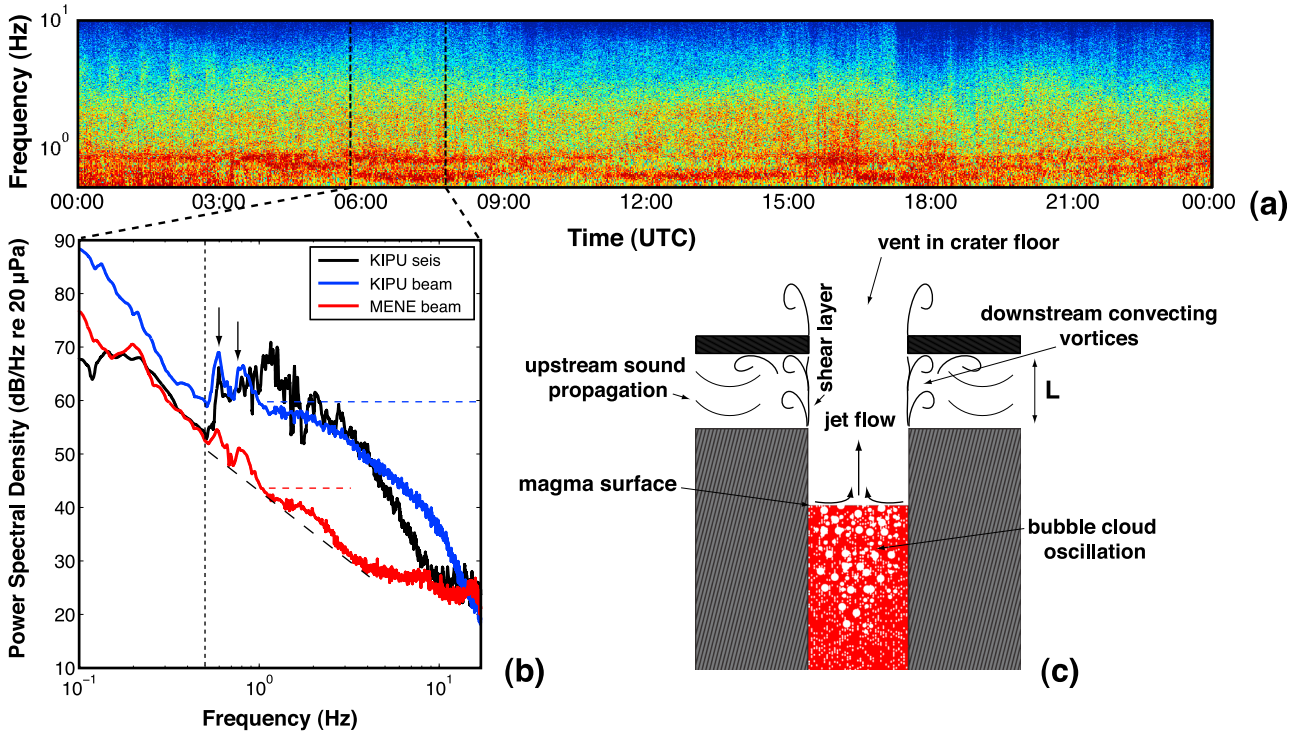

Figure 3. Tremor source considerations. (a) Log-frequency spectrogram for 24 h of beamed infrasound data from KIPU beginning at 0000 UTC Julian day 111 2007. Vertical dashed lines indicate time of data used in Figure 3b. (b) Power spectral density of beamed infrasound data at KIPU (blue) and MENE (red) expressed in dB/Hz re 20 μPa. Power spectrum of KIPU vertical seismic data (black) shown with arbitrary scale adjusted for comparison to infrasound data. Energy below ~0.5 Hz (vertical dashed line) is ambient noise (see Figure 2). There are two prominent spectral peaks at ~0.6 and ~0.8 Hz (indicated by arrows) in all data (including seismic), which exhibit complex evolution with time (Figure 3a). Additional persistent broadband infrasonic tremor is visible in KIPU data between ~0.5 and 17 Hz (band indicated by horizontal dashed blue line) and in MENE data between ~1 and 3 Hz (band indicated by horizontal dashed red line). Diagonal dashed line indicates inferred ambient noise floor at MENE. KIPU seismic data have a complicated spectrum above 0.8 Hz. (c) Schematic of infrasonic tremor source model for both broadband and harmonic components. Broadband noise may be generated by bubble cloud oscillation in a vigorously degassing magma conduit, while harmonic components may be generated by interaction of gas flow with the vent and near-surface cavities in a process analogous to the hole tone or whistler nozzle. Although depicted with infinite width, the cavity of length L would in reality be a finite volume between the magma surface and vent with resonant modes.

~9 m/s is at the upper bound of wind speeds measured at the 25 m tower at THST during the study period (Figure 2).

[10] Taken together, the KIPU and MENE data confirm the results of *Fee and Garcés* [2007], and give an indication of the propagation effects on signal power, intermittency of coherent detection, and scatter in azimuth values expected at the ~10 km range. The KIPU data suggest that such propagation effects are minimal at the ~2–3 km range. However, here we have not taken into account possible directivity effects in the source radiation and in atmospheric propagation. For instance, KIPU is in the prevailing downwind direction of Pu`u `Ō`ō and propagation effects observed in the upwind direction may be more severe. We note that the wind speed variations are diurnal between Julian days 113 and 118, but more random between Julian days 109 and 113. This illustrates the complexity of boundary layer dynamics and infrasonic propagation effects at the ~10 km range. These data will provide a reference for future studies aimed at modeling infrasonic propagation in the boundary layer.

4. Tremor Source Properties

[11] KIPU provided high signal-to-noise ratio recordings of Pu`u `Ō`ō's infrasonic tremor. We focus primarily on observations from KIPU in the remaining sections. Figure 3a shows a log-scale frequency spectrogram of time delay beamformed [*DeFatta et al.*, 1988] infrasound data at KIPU for a 24 h time period beginning at 0000 UTC Julian day 111 2007. Two distinct persistent tremor components are visible, each with different frequency content and time dependence, indicative of the continuous action of two separate physical source processes. The first component is a broadband signal concentrated between 0.5 and 15 Hz (Figure 3b). Array processing shows this to be coherent acoustic signal originating

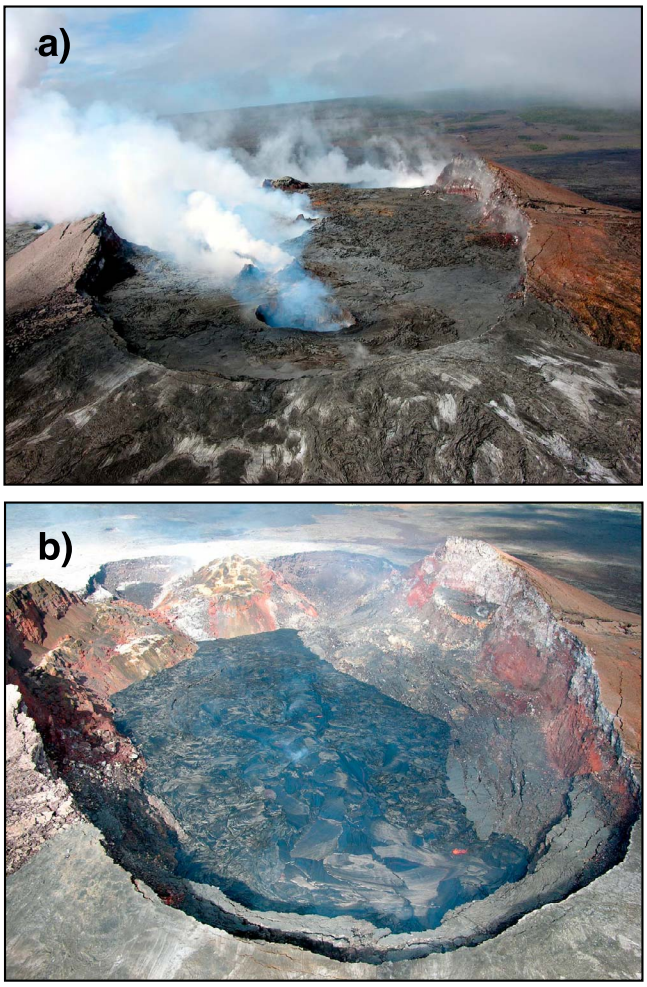

Figure 4. Photographs of the Pu`u `Ō`ō crater complex (a) on 22 February 2007 prior to our field deployment and (b) on 13 July 2007 after our field deployment. Figure 4a is representative of the state of the crater complex during our deployment, while by the time Figure 4b was taken, the solid lid within the crater complex area had collapsed and had been filled by a lava lake. View in each case is approximately from the northeast looking to the southwest. In Figure 4a, the pit in the foreground is the East Pond vent, while the steaming behind it and to the south is coming from a collection of active vents and pits in the southern portion of the Pu`u `Ō`ō crater complex, e.g., the January vent, South Wall pit and vent complex, and MLK vents and pits. The infrasonic tremor azimuths point to that general area of the crater complex but lack the azimuthal resolution to pinpoint individual vents. Photographs courtesy of U.S. Geological Survey, Hawaiian Volcano Observatory (HVO).

from the direction of the crater complex area. The second component consists of prominent spectral peaks in the ~0.6–0.9 Hz band (Figure 3b) that exhibit complex temporal dependence (Figure 3a). The relative power in the individual peaks changes with time. For example, the peak at ~0.6 Hz appears to switch on between 0600 and 0900 UTC, and again between 1200 and 1500 UTC, while the peak at ~0.8 Hz is more persistent, but switches off between 1200 and 1500 UTC (Figure 3a). Gliding or subtle changes in the frequency of these individual peaks [*Garcés et al.*, 1998] is also observed as a function of time. This signal also originates from the crater complex area and is observed throughout the KIPU deployment. Both components are recorded at MENE (Figure 3b). Although we cannot define ambient noise conditions for MENE during this time period due to the presence of the continuous tremor signal, we infer that the tremor signal lies just above the ambient noise floor at MENE (diagonal dashed line, Figure 3b).

[12] The median azimuth for the tremor signal at KIPU is ~67.0°, which points to the southern section of the Pu`u `Ō`ō crater complex. During the time of the experiment, this southern section of the crater complex contained numerous active vents and pits such as the South Wall pit and vent complex, Puka Nui vents and pit, MLK vents and pit, Beehive vent, East Pond vent, and Tephra Berm vent (http://hvo.wr.usgs.gov/). These can be seen in Figure 4a as numerous steaming openings in the southern section of the crater complex. During the experiment we were able to observe several active incandescent vents in the MLK region, and activity at the East Pond vent and Beehive vent. However, several of the areas in the South Wall complex were more difficult to access, and it is likely that multiple vents in the system could be sources of infrasound. It is therefore not clear whether one dominant vent was the primary source of infrasonic tremor, or whether the tremor resulted from the collective sum of contributions from two or possibly many more spatially distributed vents. Since no single vent seemed larger or more energetic in degassing activity than any of the other vents (Figure 4a), the latter case seems most plausible. The standard deviation of azimuths derived from PMCC for the deployment period is ~6.4°, corresponding to ~270 m distance at Pu`u `Ō`ō. Although not a formal estimate of the uncertainty in the calculated azimuth values, this standard deviation can be taken to represent the variability of calculated signal azimuth, which may result from source variability (individual spatially separated vents may have contributed more significantly to the tremor power during different times of the deployment), propagation effects (up to ~1–2° for a wind of ~9 m/s blowing perpendicular to the propagation direction), and uncertainty in the azimuth calculation as a result of noise and array response. From KIPU, the difference in azimuth between the most northerly and southerly points in the crater complex (~260 m) is ~6.2°. This is of the same order as the observed azimuthal standard deviation and indicates that we do not have the azimuthal resolution from KIPU to identify which particular vents in the crater complex acted as the main contributing tremor sources during the deployment. We note that the observed azimuthal standard deviation could also be explained by a distributed source with multiple vents in the crater complex acting as sources. To resolve individual vents within the crater complex would require a closer-range infrasonic sensor deployment [e.g., *Ripepe et al.*, 2007], which could be corroborated by infrared imaging or other thermal measurements [*Marchetti and Harris*, 2008] of the numerous active vents. This style of experiment was being planned when the new stage of Kilauea and Pu`u `Ō`ō's eruption began in June 2007 [*Poland et al.*, 2008], which included the collapse of the Pu`u `Ō`ō crater floor and the destruction of all of the

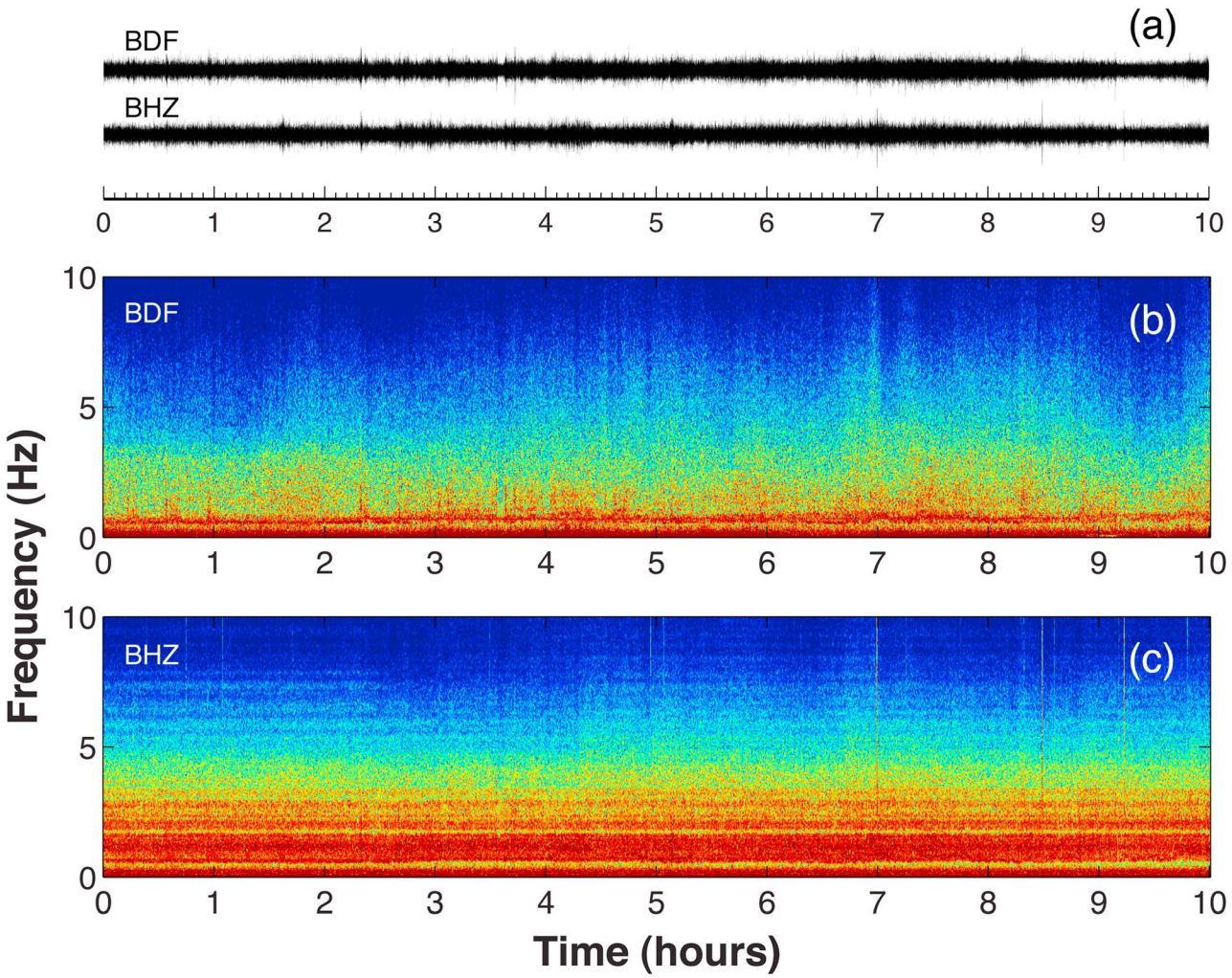

Figure 5. A comparison of 10 h of infrasonic and seismic tremor from Pu`u `Ō`ō as recorded at KIPU. Origin time is 0500 UTC Julian day 116 2007. (a) The top trace is the infrasonic beam (pressure, BDF), filtered 0.5–15 Hz; amplitude is ~0.1 Pa. The bottom trace is the vertical seismic data (velocity, BHZ), filtered 0.5–15 Hz; amplitude is ~10 μm/s. (b) Spectrogram of infrasonic beam (top trace in Figure 5a). (c) Spectrogram of seismic vertical velocity data (bottom trace in Figure 5a). In Figure 5a, infrasonic and seismic waveforms consist of a continuous signal with amplitude envelopes broadly following each another. However, there are significant differences in frequency content between the seismic (Figure 5c) and infrasonic (Figure 5b) data.

active vents and pits which presumably acted as sources in this study (Figure 4b).

5. Tremor Source Considerations

[13] The persistent tremor source under consideration is arguably highly complex. During the study period, Pu`u `Ō`ō was in a constant, elevated state of degassing in comparison to previous years [*Poland et al.*, 2008], and it is probable that this continuous degassing took the form of a roiling, bubbly lava body beneath the crater complex area. Direct observation of such a lava body was not possible in April 2007, as it was capped by a solid lid forming the crater floor (punctured by several distinct active vents, Figure 4a). However, in June 2007 deflation at Pu`u `Ō`ō, attributed to a disrupted magma supply, caused the solid crater floor to collapse by as much as 80 m [*Poland et al.*, 2008]. Shortly afterward, eruptive activity resumed and a lava lake quickly filled the crater to within 30 m of the rim (Figure 4b) [*Poland et al.*, 2008]. Furthermore, recent observations at the similar but more open Halema`uma`u vent revealed a lava body in such a state of vigorous degassing at the base of an open cavity, and similar infrasonic tremor was recorded [*Fee et al.*, 2010].

[14] Within a vigorously degassing basaltic lava system, numerous candidate acoustic source processes may be considered, including noise from turbulent lava overturning and spattering, the oscillations of bubbles [*Lu et al.*, 1990; *Chouet*, 1996], degassing noise [*Woulff and McGetchin*, 1976], resonance of gas or lava-filled cavities [*Garcés et al.*, 1998], and possibly thermoacoustic processes [*Busse et al.*, 2005; *Swift*, 2007]. A full investigation of each of these mechanisms is beyond the scope of the present study. However, one process that is likely to be important is the collective oscilla-

tions of bubble clouds within this degassing source [*Chouet*, 1996]. Bubbles act as monopole sources, and are therefore often the most efficient sound sources in flows containing them, including breaking ocean waves, waterfalls, and rivers [*Leighton*, 1994; *Park et al.*, 2008]. A turbulent liquid flow typically produces only a weak acoustic noise emission in comparison to the same turbulent liquid flow when entrained bubbles are present [*Howe*, 1998]. Due to this increased source efficiency associated with bubbles, bubble cloud oscillation seems a strong candidate for a tremor source at Pu`u `Ō`ō. In other words, if bubbles are present, they are likely to be a dominant noise source. Furthermore, bubble cloud oscillation has already been proposed as a source of seismic tremor at Pu`u `Ō`ō [*Chouet*, 1996]. Bubbles also play a critical role in the coupling between the sound field in a magma column and the atmosphere, and this is addressed in section 5.2.

[15] However, the observed sharp spectral peaks that bifurcate and glide as a function of time are more difficult to explain by a simple bubble cloud or resonator model. In section 5.3, we propose a mechanism for the production of this particular component of the tremor via the interactions of a gas jet with solid boundaries in the shallow vent structure of Pu`u `Ō`ō.

[16] We note briefly that sustained seismic tremor has long been associated with the eruption of Pu`u `Ō`ō [e.g., *Ferrazzini et al.*, 1991; *Chouet and Shaw*, 1991; *Chouet*, 1996]. Figure 5 shows 10 h of tremor from Pu`u `Ō`ō as recorded in infrasonic and seismic data at KIPU. In general, the infrasonic and seismic tremor amplitudes are correlated (Figure 5a), and some spectral characteristics are consistent between infrasonic and seismic data (Figures 5b and 5c). This suggests a related source mechanism for the seismic and infrasonic tremor. However, there are also some significant differences in the spectral content of the tremor as recorded in seismic and infrasonic data (Figures 5b and 5c). These may be a result of modification of the seismic tremor wavefield by path effects [e.g., *Goldstein and Chouet*, 1994]. In particular, our seismic sensor was located in a loosely consolidated surface layer. Alternatively, the observed spectral differences could reflect differences in how energy is radiated into the solid earth and atmosphere from a common fluid source. Given this ambiguity associated with the seismic data, we concentrate on the infrasonic observations in this study.

5.1. Bubble Cloud Oscillation

[17] An individual millimeter-scale bubble within shallow molten basalt may oscillate with a characteristic frequency of several kilohertz [*Lu et al.*, 1990; *Chouet*, 1996]. However, bubbles in a cloud are coupled oscillators, and the normal modes of bubble clouds can be much lower in frequency than those of the individual bubbles [*Lu et al.*, 1990; *Yoon et al.*, 1991]. The resonant frequency f_0 of a single bubble is approximated by [*van Wijngaarden*, 1972; *Chouet*, 1996]

$$f_0 \sim \frac{1}{2\pi}\sqrt{\frac{3P_0}{\rho_l R^2}}, \tag{1}$$

where P_0 is the static pressure in the liquid, ρ_l is the liquid density, and R is the bubble radius. In contrast, for a bubble cloud with characteristic length scale L_b we may expect eigenfrequencies

$$f_n \sim \frac{nc_{eff}}{2L_b}, \tag{2}$$

where n = 1, 2, 3, …, and c_{eff} is the effective sound speed of the liquid-bubble mixture, given by Wood's equation [*Wood*, 1964]:

$$c_{eff} = \left\{\left[(1-\phi)\rho_l + \phi\rho_g\right]\left[(1-\phi)\kappa_l + \phi\kappa_g\right]\right\}^{-1/2}, \tag{3}$$

where ϕ is the void fraction (gas-volume fraction), ρ_g is the density of the gas, and κ_l and κ_g are the compressibilities of the liquid and gas, respectively. Considering that $\rho_l \gg \rho_g$ and $\kappa_l \ll \kappa_g$, equation (3) can be approximated as [e.g., *van Wijngaarden*, 1972; *Wilson and Roy*, 2008]

$$c_{eff} \sim \sqrt{\frac{\nu P_0}{\rho_l \phi(1-\phi)}}, \tag{4}$$

where ν is the polytropic index of the gas in the bubble. For ϕ in the range 10^{-4} to 10^{-1}, and considering that $\nu \sim 1$, equation (4) further reduces to [e.g., *Lu et al.*, 1990; *Chouet*, 1996; *Hahn et al.*, 2003]

$$c_{eff} \sim \sqrt{\frac{P_0}{\rho_l \phi}}. \tag{5}$$

Assuming $\phi \sim (R/L_b)^3 N$, where N is the number of bubbles in the cloud, combining equations (1), (2), and (5) gives the ratio f_n/f_0 as [*Lu et al.*, 1990; *Chouet*, 1996]

$$\frac{f_n}{f_0} \sim \frac{n}{\phi^{1/6} N^{1/3}}. \tag{6}$$

For instance, *Chouet* [1996] illustrated that a single bubble in shallow liquid basalt with $R \sim 1$ mm, $\rho_l \sim 2500$ kg/m^3 and $P_0 \sim 2.5$ MPa (depth $z \sim 100$ m for $P_0 = \rho_l g z$ where g is the acceleration due to gravity) may oscillate at $f_0 \sim 10$ kHz (equation (1)). In contrast, a bubble cloud in basalt of the same density and pressure, with characteristic length scale $L_b \sim 50$ m, void fraction $\phi \sim 10^{-2}$, and constant individual bubble radius $R \sim 1$ mm may radiate at a frequency of $f_1 \sim$ 2 Hz (equation 6), which is in agreement with the infrasonic frequencies observed. We hypothesize that noise from bubble cloud oscillation is the source of broadly peaked tremor between 0.5 and 17 Hz. Whereas the turbulent overturning of lava would itself be an inefficient sound source, this turbulence may play a role in driving the collective oscillations of bubbles. A random arrangement of bubbles with various radii within a heterogeneous pressure and flow field may result in a continuous emission of low-frequency broadband noise in contrast to the harmonic series defined in equation (2).

[18] Bubble cloud oscillation has typically been investigated in water [*Commander and Prosperetti*, 1989; *Lu et al.*, 1990; *Yoon et al.*, 1991; *Park et al.*, 2008], where the effect of liquid viscosity is negligible. *Ichihara and Kameda* [2004] extended the theory to include the effects of liquid viscosity and volatile diffusion on bubble oscillation in magma. They found that attenuation and dispersion of pressure waves in magma are severe for frequencies lower than the charac-

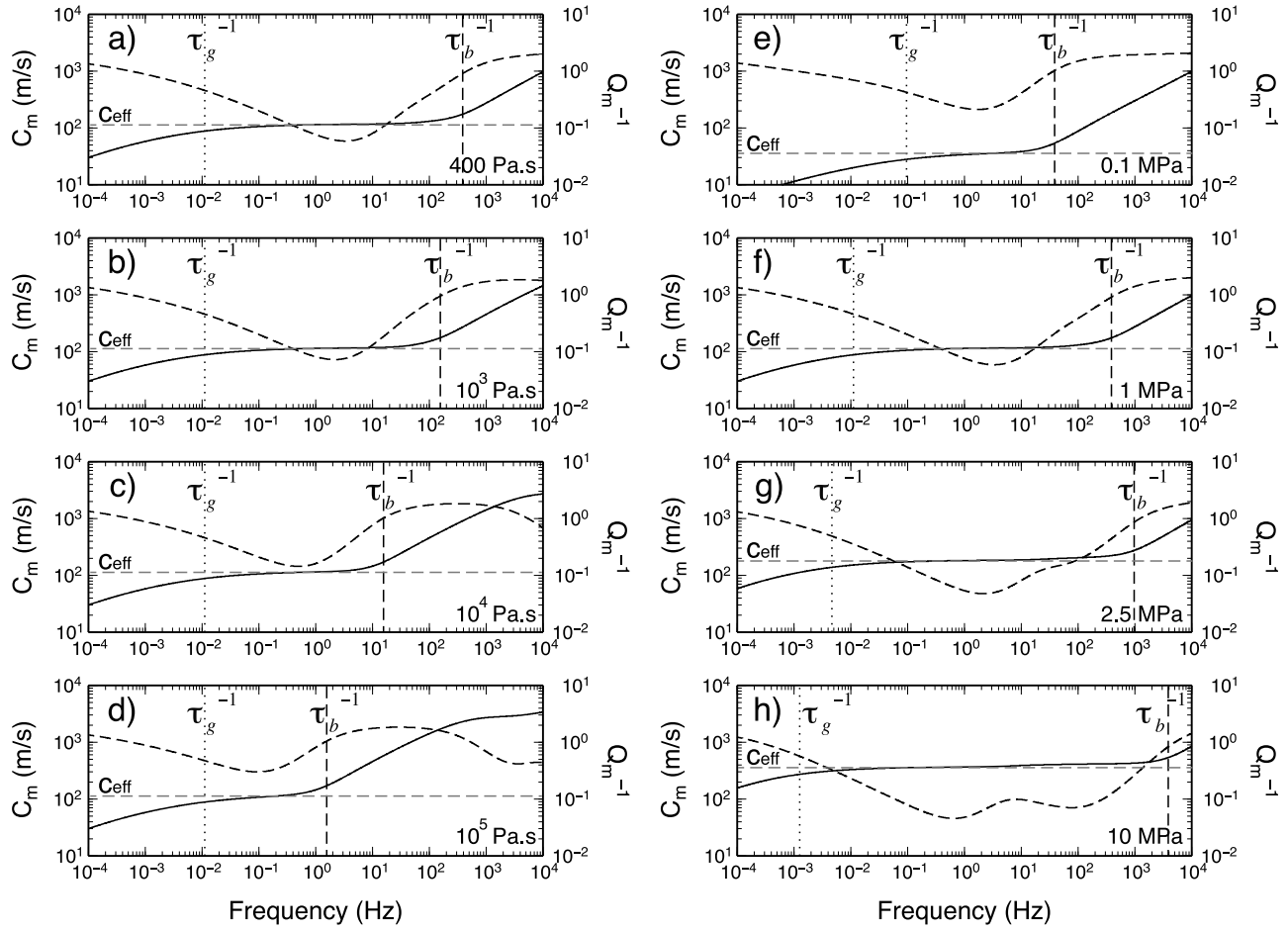

Figure 6. Sound speed c_m (m/s) (left axis, solid curve) and attenuation Q_m^{-1} (right axis, dashed curve) of pressure waves in a bubbly liquid including effects of volatile diffusion and melt viscosity according to the model of *Ichihara and Kameda* [2004]. The material parameters are those assumed for H_2O vapor in basalt at a temperature of 1273 K by *Ichihara and Kameda* [2004, Figures 6 and 7]. In Figures 6a–6d, the hydrostatic pressure is set to 1 MPa and the viscosity is varied: (a) 400 Pa s, (b) 10^3 Pa s, (c) 10^4 Pa s, and (d) 10^5 Pa s. In Figures 6e–6h, the viscosity is held at 400 Pa s and the hydrostatic pressure is varied: (e) 0.1 MPa (depth ~4 m assuming $\rho_l = 2600$ kg/m^3), (f) 1 MPa (depth ~40 m), (g) 2.5 MPa (depth ~ 100 m), and (h) 10 MPa (depth ~ 400 m). The horizontal dashed gray line indicates the effective sound speed c_{eff} (equation (5)). The characteristic frequencies (in Hz) for volatile diffusion (τ_g^{-1}, vertical dotted line) and viscous effects on bubble expansion (τ_b^{-1}, vertical dashed line) are also shown. In the frequency range between these two characteristic frequencies $\tau_g^{-1} \le f \le \tau_b^{-1}$, attenuation and dispersion due to viscosity and volatile diffusion are small and the sound speed c_m agrees with the effective sound speed c_{eff}. The effects of viscosity and volatile diffusion are therefore negligible in the frequency band 0.5–17 Hz of the observed tremor (Figure 3) for the parameters used here according to the model of *Ichihara and Kameda* [2004].

teristic frequency τ_g^{-1} of mass transfer into and out of the bubbles by diffusion of volatiles, or close to the characteristic frequency τ_b^{-1} of the viscous response of the bubble in the magma. Such effects could also inhibit the tremor source outlined above, as they may inhibit cloud oscillation and thus prevent the bubbles from generating sound. These effects have negligible influence in the frequency range $\tau_g^{-1} \le f \le \tau_b^{-1}$ where here τ_g^{-1}, τ_b^{-1} and f are frequencies in Hz. The time scale for volatile diffusion τ_g is given by [*Ichihara and Kameda*, 2004]

$$\tau_g = \frac{2\pi R^2}{9\kappa_{gl}} \left(\frac{\rho_l P_0}{\rho_g} \frac{\partial C_{eq}}{\partial P} \right)^{-2}, \tag{7}$$

where κ_{gl} is the diffusivity of the volatile in the liquid and $C_{eq}(P)$ is the equilibrium volatile concentration at pressure P. The bubble volume relaxation time τ_b due to melt viscosity is given by

$$\tau_b = \frac{8\pi\eta_0}{3K_g}, \tag{8}$$

where η_0 is the melt shear viscosity, and K_g is the bulk modulus of the bubble for an adiabatic process with $K_g = \gamma P_0$, where γ is the ratio of specific heats, $\gamma \sim 1.3$ [*Ichihara and Kameda*, 2004]. We note that here we are considering the raw melt viscosity η_0 of the liquid magma, and not the effective viscosity η_{eff} of the bubbly mixture. The effective vis-

cosity of a bubbly mixture increases with the void fraction ϕ, and is the relevant parameter when dealing with bulk properties of the fluid, such as the attenuation of an acoustic wave passing through the bubbly mixture [*Garcés*, 1997, 2000; *Marchetti et al.*, 2004]. The raw melt viscosity is the viscosity experienced by the individual bubbles oscillating within the melt. Note that this assumes a relatively low void fraction where bubbles do not touch (i.e., we are assuming that the magma-gas mixture is not a foam). The importance of effective viscosity for the propagation of the sound field in a magma column to the atmosphere is addressed in section 5.2.

[19] Following the procedure and assumptions described by *Ichihara and Kameda* [2004], we first assume $R \sim 1$ mm, $\kappa_{gl} \sim 10^{-9}$ m^2/s, $\rho_l \sim 2600$ kg/m^3 and $P_0 \sim 1$ MPa, and we use the values in Table 1 of *Ichihara and Kameda* [2004] for the quantity $A_g = (\rho_l P_0/\rho_g)(\partial C_{eq}/\partial P)$ in equation (7) assuming H_2O vapor at a temperature of 1273 K for the gas phase. This yields a characteristic frequency for volatile diffusion $\tau_g^{-1} \sim 0.01$ Hz, which is much lower than the frequencies of infrasonic tremor considered (0.5–17 Hz), suggesting that the effect of volatile diffusion can be neglected. The melt viscosity η_0 may be ~400 Pa s for shallow molten basalt (*Shaw* [1972]; following *Vergniolle and Brandeis* [1996]), yielding a value of $\tau_b^{-1} \sim 1$ kHz. This is much higher than the infrasonic tremor frequencies considered, indicating that the effect of a viscous melt may also be neglected for this value of viscosity. However, given the poor constraints on melt viscosity at Pu`u `Ō`ō of which we are aware, and the fact that melt viscosity is a strong function of water content [*Shaw*, 1972], it is important to investigate the effects of a larger range of melt viscosity.

[20] A more thorough investigation of variations in melt viscosity and magmastatic pressure is presented in Figure 6. Figure 6 shows the sound speed and attenuation of pressure waves in a liquid-bubble mixture according to the model of *Ichihara and Kameda* [2004] for different values of the melt viscosity η_0 and magmastatic pressure P_0. *Ichihara and Kameda* [2004] employ a linear viscoelastic rheology for the melt [*Webb*, 1997], in which the shear and bulk moduli of the viscoelastic material are complex functions of the frequency of an applied sinusoidal oscillation. As in the work of *Ichihara and Kameda* [2004], we assume an unrelaxed bulk modulus $K_\infty = 30$ GPa, an unrelaxed shear modulus $\mu_\infty = 10$ GPa and a relaxed bulk modulus $K_0 = 20$ GPa for the parameters describing the linear viscoelastic rheology [*Webb*, 1997]. We further assume that the void fraction $\phi = 0.03$ (compare with Figures 6 and 7 of *Ichihara and Kameda* [2004]). In Figures 6a–6d, the magmastatic pressure is held fixed at 1 MPa (~40 m depth assuming a magma density $\rho_l = 2600$ kg/m^3) while the melt viscosity is varied at 400, 10^3, 10^4, and 10^5 Pa s. The characteristic frequencies τ_g^{-1} and τ_b^{-1} are also shown. In the frequency range between these two characteristic frequencies, $\tau_g^{-1} \leq f \leq \tau_b^{-1}$, attenuation and dispersion due to melt viscosity and volatile diffusion are small, and the sound speed of the liquid-bubble mixture agrees with the effective sound speed (equation (5)) [*Ichihara and Kameda*, 2004]. Between these characteristic frequencies we also assume that the effects of volatile diffusion and melt viscosity on the oscillation of bubbles are small, so that bubble clouds could oscillate freely and produce tremor. Here we find that for a depth of ~40 m in a basaltic conduit, a melt viscosity several orders of magnitude higher than 400 Pa s, i.e., $\eta_0 \sim 10^4$–10^5 Pa s is necessary to lower τ_b^{-1} into the observed frequency range (0.5–17 Hz) and to make viscous effects important in this analysis.

[21] In Figures 6e–6h the melt viscosity is instead held fixed at 400 Pa s while the magmastatic pressure is now varied at 0.1 MPa (depth ~4 m), 1 MPa (~40 m), 2.5 MPa (depth ~ 100 m), and 10 MPa (depth ~ 400 m). These figures indicate that for a melt viscosity of 400 Pa s, τ_g^{-1} and τ_b^{-1} are outside of the observed tremor frequency range (0.5–17 Hz) except in the upper few meters of the conduit. We find that further investigation using the same values of pressure but for different values of viscosity supports the conclusion from Figures 6a–6d that a melt viscosity on the order of ~10^4–10^5 Pa s would be required to bring τ_g^{-1} and τ_b^{-1} into the observed tremor frequency range for the shallowest section of the conduit. We note, however, that bubble growth would be most vigorous close to the magma surface where pressure is lower, and with increasing depth in the magma column the increased pressure would inhibit bubble growth and oscillation [*Marchetti et al.*, 2004]. Radiation of the sound field from the magma into the atmosphere would also be most efficient with a very shallow source location, i.e., within a few tens of meters of the magma surface (Figure 3c) [*Garcés et al.*, 1998; *Marchetti et al.*, 2004; *Godin*, 2006], and this is discussed in the following section.

5.2. Coupling Between the Sound Field in a Magma Conduit and the Atmosphere

[22] Of critical concern in volcano acoustics is the coupling of the sound field in a magma column to the atmosphere. In a canonical investigation of this phenomenon, *Buckingham and Garcés* [1996] proposed that the magma surface may be treated as a pressure release boundary due to the strong impedance contrast between the two media. This is also conventional in ocean acoustics (the ocean surface is generally treated as a pressure-release boundary). In the work by *Buckingham and Garcés* [1996], weak radiation into the atmosphere of the resonant sound field trapped in a magma conduit was possible due to the diaphragm-like vertical motion of the magma surface acting as a piston set in an infinite baffle (compare a loudspeaker cone). Later, *Garcés and McNutt* [1997] and *Garcés et al.* [1998] proposed that a region of low sound speed close to the magma surface corresponding to a bubbly mixture with high void fraction (see equation (5)) may lower the impedance contrast between the magma and atmosphere, and enable more efficient radiation of sound into the atmosphere. However, a region of high void fraction would also have a high effective viscosity η_{eff}:

$$\eta_{eff} = \frac{3}{4}\eta_b + \eta_s, \tag{9}$$

where η_b is the bulk viscosity and η_s is the shear viscosity, and both η_b and η_s are nonlinear functions of the void fraction [*Garcés*, 1997, 2000; *Marchetti et al.*, 2004]. *Marchetti et al.* [2004] showed that a basaltic melt with viscosity $\eta_0 \sim 500$ Pa s, but a high void fraction ($\phi > 0.4$), could have an effective viscosity $\eta_{eff} \sim 10^4$–10^5 Pa s close to the magma surface, resulting in strong attenuation of acoustic waves. *Marchetti et al.* [2004] proposed that such attenuation would limit the ability of sound sources deep in a bubbly magma

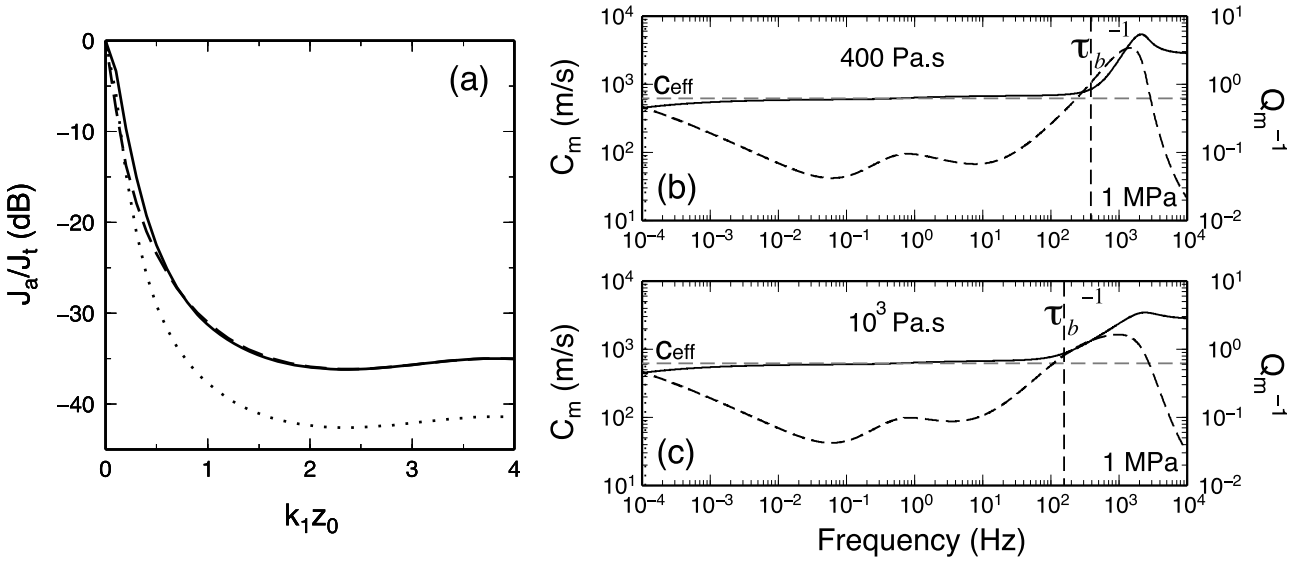

Figure 7. (a) Transparency (J_a/J_t in dB) for a monopole source at depth z_0 below a liquid-air interface with wave number in the liquid $k_1 = 2\pi/\lambda$ [*Godin*, 2006, 2007] for water (c_w = 1500 m/s, ρ_w = 1000 kg/m^3, solid line, compare with Figure 4 of *Godin* [2006]), bubbly magma (c_{eff} = 620 m/s, ρ_l = 2600 kg/m^3, dotted line), and liquid magma with no gas (c_{eff} = 2500 m/s, ρ_l = 2600 kg/m^3, dashed line). Energy within $k_1z_0 \sim 1$ of the surface is propagated efficiently into the atmosphere due to inhomogeneous waves. (b and c) Sound speed c_m (m/s) (left axis, solid curve) and attenuation Q_m^{-1} (right axis, dashed curve) of pressure waves in a bubbly liquid [*Ichihara and Kameda*, 2004], where bubble radius $R \sim 1$ cm and void fraction $\phi \sim 0.001$, the pressure and viscosity are indicated on the plots, and all other parameters are as in Figure 6. The effective sound speed c_{eff} is ~620 m/s and is a good approximation to the sound speed in the frequency range of the observed tremor. This value of c_{eff} used in Figure 7a is therefore justified.

conduit to radiate to the atmosphere. However, sound sources in the uppermost conduit section could be coupled to the atmosphere.

[23] Recent theoretical work [*Godin*, 2006, 2007] on the boundary at the ocean surface may have important implications for this problem in volcano acoustics. *Godin* [2006, 2007] showed that, contrary to conventional wisdom, the interface between a liquid with high sound speed (e.g., the ocean with sound speed ~1500 m/s) and the overlying atmosphere (sound speed ~330 m/s) is in fact anomalously transparent to low-frequency sound. Whereas high-frequency ray theory predicts that only a negligible amount of sound could be transmitted from the ocean into the atmosphere, *Godin* [2006, 2007] showed that almost all of the energy at infrasonic frequencies can be transmitted for shallow sources (i.e., sources within approximately one wavelength of the ocean surface) due to the role of inhomogeneous waves. This phenomenon could enable the shallow sound field in a magma column to radiate efficiently into the atmosphere without the need for a high void fraction and low sound speed layer.

[24] For instance, suppose that we now have a relatively low void fraction $\phi \sim 10^{-3}$ near the magma surface, a bubble radius $R \sim 1$ cm, and a bubble cloud with characteristic length scale $L_b \sim 50$ m. The value of R was chosen to give a value of f_1 (equation (6)) in the range of the observed infrasonic tremor for this low value of ϕ; i.e., this would correspond to $N \sim 10^8$ bubbles, or ~240 bubbles/m^3 assuming $\phi \sim \frac{4}{3}\pi R^3 N/V$, where V is the volume 1 m^3. In this case, equation (1) with $P_0 \sim 1$ MPa and $\rho_l \sim 2600$ kg/m^3 yields $f_0 \sim 540$ Hz, equation (5) yields $c_{eff} \sim 620$ m/s, and equation (6) yields $f_1 \sim 3$ Hz. We note that bubbles with the larger radius of 1 cm used here would also probably result in more powerful sound production than the radius of 1 mm used in the previous section, although a quantitative assessment of the sound power output from volcanic bubble clouds is beyond the scope of the present study. The sound speed $c_{eff} \sim 620$ m/s compared to the atmospheric sound speed $c_a \sim 330$ m/s, together with the density $\rho_l \sim 2600$ kg/m^3 compared to the atmospheric density $\rho_a \sim 1.2$ kg/m^3 result in a large impedance mismatch ($\rho_l\, c_{eff}/\rho_a\, c_a$), which according to high-frequency theory would result in poor acoustic transmission from the magma to the atmosphere. However, in Figure 7a we show the acoustic transparency J_a/J_t of this magma-air surface (c_{eff} = 620 m/s, ρ_l = 2600 kg/m^3, dashed line, Figure 7a), where J_a is the acoustic power flux into the atmosphere from a monopole source in the liquid and J_t is the total power output of the source, calculated according to *Godin* [2006, 2007]. The transparency is plotted against the nondimensional source depth $k_1\, z_0$, where k_1 is the wave number of the acoustic wave in the liquid (wave number $k = 2\pi\, f/c$), and z_0 is the source depth. For comparison, we also show the transparency for the ocean-air surface (c_w = 1500 m/s, ρ_w = 1000 kg/m^3, solid line, Figure 7a) and the surface of liquid magma with no gas (c_l = 2500 m/s [*Garcés et al.*, 1998], ρ_l = 2600 kg/m^3, dotted line). We find that, as in the ocean environment, anomalous transparency is predicted for the magma-air surface for $k_1z_0 < 1$. For c_{eff} = 620 m/s and frequency ~ 3 Hz this would correspond to a depth ~ 30 m, whereas for c_{eff} = 2500 m/s this would cor-

respond to a depth of 132 m. This indicates that the sound field radiated by oscillating bubbles within the upper few tens of meters in a bubbly magma column may be propagated into the atmosphere via anomalous transparency without requiring a low sound speed and high void fraction, while anomalous transparency may be expected up to a greater depth in a degassed conduit with higher sound velocity. In Figures 7b and 7c we show the curves for c_m and Q_m^{-1} predicted by the model of *Ichihara and Kameda* [2004] for the parameters used for the bubbly magma here. Figures 7b and 7c justify the use of $c_{eff} \sim 620$ m/s and the neglect of melt viscosity and volatile diffusion effects on bubble oscillation for the parameters considered above.

[25] Taken together with the results of section 5.1, this suggests that the collective oscillations of a cloud of small bubbles (R of millimeters up to centimeters) within the upper few tens of meters of a magma column with melt viscosity ~ 400–1000 Pa s may be an efficient source of sound into the atmosphere. Anomalous transparency of the magma-air interface may allow the transmission of the low-frequency sound field in the magma conduit into the atmosphere, without requiring a large void fraction near the magma surface. This transparency effect would be reduced at high frequencies (Figure 7a). However, the void fraction may inevitably rise sharply in the upper few meters of a magma conduit. In this case, effective viscous attenuation effects may act on the higher frequencies of observed tremor [*Garcés*, 1997, 2000; *Marchetti et al.*, 2004]. Such frequency-dependent effects of liquid-bubble mixtures and the magma-air acoustic transmission may partially explain why the observed tremor power spectrum is peaked between ~ 1 and 3 Hz, and acoustic power is reduced at higher frequencies (Figure 3a). We note that this general view of the continuous degassing process (i.e., vigorous degassing taking place within the upper few tens of meters of a conduit) is consistent with that proposed by *Edmonds and Gerlach* [2007] based on measurements of volcanic gas composition at Pu`u `Ō`ō in 2004–2005 using open path Fourier transform infrared spectroscopy.

[26] This proposed mechanism for the generation of continuous Hawaiian infrasonic tremor can also be related to models for more impulsive infrasonic signal production by moderate to large bubble bursts observed in numerous Strombolian and Hawaiian systems [*Vergniolle and Brandeis*, 1996; *Ripepe et al.*, 2007; *Johnson et al.*, 2008; *Gerst et al.*, 2008; *Fee et al.*, 2010]. The difference being that to generate an observable impulsive signal, small bubbles must coalesce into larger bubbles, which eventually explode energetically at the lava surface with high overpressure [*Johnson et al.*, 2008; *Gerst et al.*, 2008]. *Ripepe et al.* [2007] observed numerous small-amplitude impulsive signals at Stromboli Volcano which were more persistent and lower in amplitude than typical Strombolian explosion signals. They attributed these signals to the persistent bursting of relatively small bubbles at the top of the magma column in contrast to the larger bubble bursts that generate the typical explosion signals. The proposed system for Pu`u `Ō`ō's broadband infrasonic tremor can be thought of as an end-member of this spectrum of processes, where the tremor is generated by a population of bubbles that have not coalesced into large exploding bubbles, and are driven into continuous oscillation by lava motion. Continuous bursting of the bubbles at the lava surface would provide a continuous flux of gas. The ascent of this gas through near-surface cavities to the atmosphere is discussed in the following section.

5.3. Self-Sustained Shear Layer Oscillations

[27] Although bubbles offer a promising mechanism for the production of broadband infrasonic tremor in a shallow magma conduit, it is difficult to explain the observed sharply peaked harmonic tremor component with the same model. The sharply peaked harmonic tremor in the ~0.6–0.9 Hz band has a spectral signature and temporal dependence distinct from the broadband signal, and likely results from a separate physical process (Figure 3). Sharply peaked spectra in volcanic seismic and acoustic signals are usually attributed to resonance in fluid-filled cavities. However, the physics of the driving mechanisms (trigger mechanisms) sustaining the resonance for long-duration tremor sources remains poorly understood [*Chouet*, 1996]. One type of self-sustained oscillation that may be relevant to the harmonic tremor source at Pu`u `Ō`ō is that which results from the aeroacoustic interaction of the shear layer of a low-velocity gas jet with a solid boundary. *Rockwell and Naudascher* [1979] provide a comprehensive summary of the phenomena of discrete acoustic frequencies (tones) produced by shear layers impinging on solid objects. Since there are different types of shear layers (i.e., jets and mixing layers of various geometries) and many possibilities for the geometry of the solid boundaries (e.g., edges, holes, rings, plates, flaps, and cavities), these interactions give rise to a diverse family of processes with common characteristics and similar underlying physical mechanisms. This family of processes includes the edge tone, which results from the impingement of a planar jet on a solid edge [*Nyborg et al.*, 1952], periodic noise produced by airflow (i.e., a mixing layer) over a rectangular cavity [*Rossiter*, 1964], the hole tone, which is produced by the flow of an axisymmetric jet from one plate impinging on a second plate with a hole in it [*Chanaud and Powell*, 1965; *Langthjem and Nakano*, 2005], and many other possible configurations [*Rockwell and Naudascher*, 1979]. Each of these processes is thought to involve a similar complex feedback mechanism. When the flow encounters the solid object, it is impeded slightly and a hydrodynamic or acoustic disturbance is sent back upstream where it then interacts with a sensitive area of the shear layer upstream to create vortices. These vortical oscillations in the shear layer then propagate downstream again, forming a closed feedback loop and self-sustained oscillations at specific frequencies [*Rockwell and Naudascher*, 1979]. The frequencies f of tones produced are nondimensionalized as the tonal Strouhal number $St = fL/U$, where L is the length scale of the feedback process and U is the free-stream velocity. For instance, L can be the length of the cavity or distance from the jet nozzle to the solid object, and U the mean flow-velocity of the jet in the absence of the solid boundary. The Strouhal numbers of the resulting acoustic signals were found empirically by *Rossiter* [1964] to agree with

$$St_m = \frac{(m-\gamma)}{\left(\frac{1}{K}+M\right)}, \tag{10}$$

where m is a mode number, $m = 1, 2, 3, \ldots, M$ is the Mach number ($M = U/c_0$, where U is the free-stream velocity

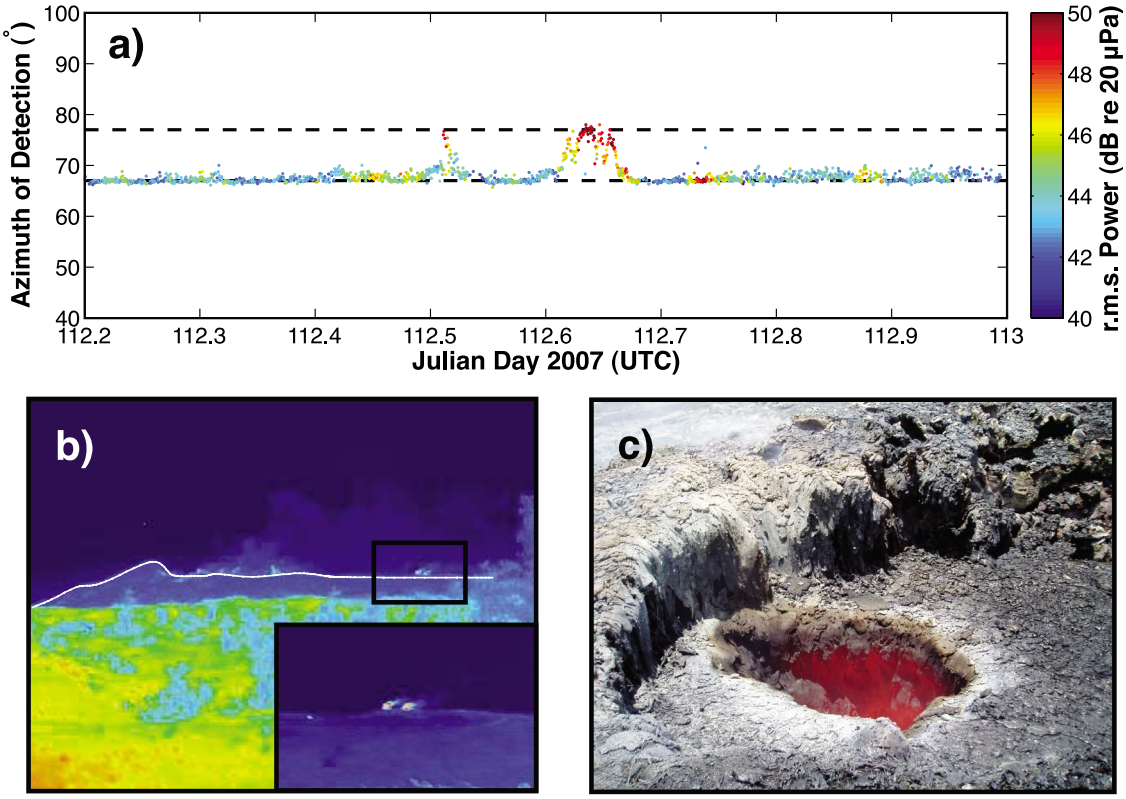

Figure 8. Infrasonic signal variation associated with lava tube activity as corroborated by audible noises and infrared imaging. (a) The 5–10 Hz band PMCC processing during Julian day 112.2–113 2007. Note that coherent signal detection azimuths deviate from that of the crater complex and begin to arrive from the greater azimuth of ~77°. This coincides with the time in which audible noises were heard coming from that approximate direction. The crater complex source at ~67° does not end during these times but is no longer the dominant sound source in the 5–10 Hz band. PMCC array processing is unable to differentiate between the two competing signals during these times. (b) Infrared image taken from KIPU array location toward Pu`u `Ō`ō, revealing incandescent sources to the south of the main crater complex. White line indicates approximate topography of Pu`u `Ō`ō. Area in box is expanded in the inset. In inset, right-hand incandescent source corresponds to new lava tube skylight described in text. Left-hand incandescent source is the acoustically quiescent kiln hornito. (c) New skylight vent (corresponding to right-hand source in Figure 8b) from which the infrasound and audible sounds originated, photographed on Julian day 115 2007.

of the flow and c_0 is the sound speed), and K and γ are empirical constants, K, $\gamma < 1$. Equivalently, the observed frequencies of oscillation or Rossiter modes can be expressed as

$$f_m = \frac{U}{L}\frac{(m-\gamma)}{\left(\frac{1}{K}+M\right)}. \tag{11}$$

Rossiter [1964] further proposed that the constant K corresponds to the ratio of the vortex convection velocity U_c to the free-stream velocity, i.e., $U_c = KU$, and K is typically around ~0.4–0.6 for most processes [*Howe*, 1998]. γ remains an empirical constant, interpreted as a phase lag. The phase lag is due to both (1) the time delay between the vortex impingement on the solid boundary and the emission of the acoustic/hydrodynamic disturbance, and (2) the delay between the arrival of the acoustic/hydrodynamic disturbance at the upstream shear layer and the release of new vortices. Equation (11) can therefore be expressed in terms of the physical parameters of the system:

$$\frac{L}{U_c}+\frac{L}{c_0}=\frac{(m-\gamma)}{f_m}, \tag{12}$$

which is known as Rossiter's equation [*Howe*, 1998]. Here, the quantity L/U_c represents the time taken for a vortex to travel downstream from the source to the impingement object, and L/c_0 is the time taken for the acoustic disturbance to travel upstream from the impingement object to the vortex source. *Delprat* [2006] has further proposed that by setting $m = 1$ and $\gamma = 0$, equation (12) can be expressed in terms of the fundamental aeroacoustic loop frequency f_a of the feedback process:

$$\frac{L}{U_c}+\frac{L}{c_0}=\frac{1}{f_a}. \tag{13}$$

The phase shift γ in equations (11) and (12) then results in the observed Rossiter mode frequencies f_m being offset from integer multiples of the aeroacoustic loop frequency f_a, as $f_m = (m - \gamma)f_a$ [*Howe*, 1998; *Delprat*, 2006].

[28] Several of the shear layer and solid object impingement geometries that can result in tone production [*Rockwell and Naudascher*, 1979] may be appropriate to volcanic settings. In particular, the edge tone [*Nyborg et al.*, 1952], hole tone [*Chanaud and Powell*, 1965], and jet flow through flaring horns [*Hirschberg et al.*, 1989] could be considered as small laboratory-scale analogs for volcanic degassing past solid vent walls, through near-surface cavities, and from a vent set in an upward flaring crater, respectively. Since the spatial scales for a volcano are large, a similar aeroacoustic flow process operating with the same *St* but at a volcanic length scale could produce low-frequency (infrasonic) acoustic radiation.

[29] The hole tone geometry seems particularly appropriate to the vent geometry at Pu`u `Ō`ō in April 2007 (Figures 4a and 8c). The hole tone, also known as the Rayleigh bird call [*Rayleigh*, 1976], is generated in the laboratory when an axisymmetric jet issuing from a nozzle in a plate impinges on a second plate with a hole in it [*Chanaud and Powell*, 1965]. The jet continues through the hole in the second plate but is impeded slightly as it does so, resulting in the impingement disturbance. The acoustic disturbance propagates back upstream where it interacts with the jet near the nozzle outlet, and the resultant vortical oscillations propagate back downstream toward the second plate, and so on. A common example of this phenomenon is a whistling tea kettle. It is conceivable that a similar process could have occurred within the shallow degassing region underneath the crater complex of Pu`u `Ō`ō if a similar geometry were present (Figure 3c).

[30] In applying equation (13) to the hole tone, L is the length scale between the jet outlet and the second hole or vent (Figure 3c), and $U_c = KU$ where U is the mean jet velocity and K is estimated at ~0.6–0.7 from laboratory experiments [*Langthjem and Nakano*, 2005]. Suppose a low-velocity gas jet streams from a vent overlying a magma conduit, travels through a small near-surface cavity, and escapes through a second vent in the overlying crater floor (Figure 3c). This gas jet may consist of volatiles escaping the magma in addition to locally entrained air. A similar geometry consisting of a vigorously convecting lava body at the base of a subsurface cavity which opens to the atmosphere has been observed recently at the more accessible Halema`uma`u vent [*Fee et al.*, 2010], and this type of geometry also seems reasonable for several of the active vents at Pu`u `Ō`ō during April 2007 (e.g., see Figure 8c). For Pu`u `Ō`ō, let the distance from jet origin to the vent be $L \sim 15$ m, the mean jet flow speed may be $U \sim 8$ m/s, which gives $U_c \sim 0.65 \times 8 \sim 5$ m/s. Then for a dominantly steam-filled cavity with sound speed $c_0 \sim 450$ m/s [*Fee et al.*, 2010] we obtain the fundamental aeroacoustic loop frequency $f_a \sim 0.33$ Hz. Since a reasonable value for γ is 0.25 for a wide range of flow conditions [*Rossiter*, 1964], the first three Rossiter modes are given by $f_m = (m - 0.25)f_a$ for $m = 1, 2, 3$, yielding $f_1 \sim 0.25$ Hz, $f_2 \sim 0.6$ Hz, and $f_3 \sim 0.9$ Hz. The values for f_2 and f_3 from this simple discussion are roughly consistent with the observed frequencies of sharply peaked harmonic tremor (Figure 3b), suggesting that a process similar to the hole tone is a plausible source for the observed infrasonic tremor. We note that the constants γ and K can vary spatially and with Mach number [*Malone et al.*, 2009] indicating that other physically plausible values for the length L and jet flow speed U could lead to a better match to the observed infrasonic frequencies. Rossiter's equation is useful for predicting possible excitation frequencies, but does not predict which particular frequencies will be excited or the most dominant tones in a given system [*Malone et al.*, 2009]. In particular, absence of the fundamental mode $f_1 \sim 0.25$ Hz predicted in our analysis would not be surprising [*Malone et al.*, 2009].

[31] The Rossiter modes are not usually integer harmonics of a fundamental frequency, and in general do not correspond to acoustic modes of the cavity [*Howe*, 1998; *Delprat*, 2006]. Nevertheless, resonators can exert their influence on self-sustained shear layer tones to create more stable spectral peaks [*Nyborg et al.*, 1952; *Rockwell and Naudascher*, 1978]. For instance, if there is a resonant pipe or Helmholtz cavity in the section L through which a jet flows, the dominant Rossiter mode tends to coincide with the acoustic or Helmholtz cavity modes, and the sound output at these frequencies is particularly high. This type of process occurs in the "whistler nozzle" phenomenon thought to be responsible for human whistling [*Hussain and Hasan*, 1983; *Wilson et al.*, 1971]. In this case, both the cavity modes (Helmholtz or acoustic modes) and the jet dynamics are important in sustaining the tone. The gap of length L depicted in Figure 3c could be generated by a process such as a solid lid forming over the lava, and the subsequent fall of the lava level. In reality this would form a finite cavity, the resonant properties of which would influence the frequency of sound produced. We note that *Julian* [1994] proposed a mechanism of continuous tremor excitation by self-sustained oscillations resulting from fluid flow through a conduit with elastic walls. The model of *Julian* [1994] is somewhat analogous to the mechanism of tone excitation in a clarinet, where vibrations of the elastic walls of the conduit are analogous to the vibrations of the reed in a clarinet mouthpiece [*Fletcher*, 1999; *Fletcher and Rossing*, 2008]. The mechanism discussed here is more analogous to that in reedless musical instruments such as the flute, where the interaction of an air jet from the player's lips with a solid edge in the mouthpiece generates edge tones which are coupled closely to the resonant modes of the flute cavity [*Fletcher*, 1999; *Fletcher and Rossing*, 2008].

[32] One general qualitative characteristic of flow-induced oscillations caused by jet shear layers impinging on solid objects is that the oscillation frequencies can change depending on the length scale L or the flow speed of the jet U, and can exhibit sudden discontinuous frequency jumps [*Rockwell and Naudascher*, 1979]. The various stable modes of operation between the frequency jumps are referred to as *stages*, and several stages and their harmonics can exist simultaneously [*Nyborg et al.*, 1952]. In this framework, the complex time evolution (e.g., gliding and mode switching) of frequency peaks of the observed tremor may relate to fluctuations in gas velocity U issuing from the vent and the transition between different stages. L could also change if the lava level were to fluctuate up and down. In the multi-vent Pu`u `Ō`ō system it is also possible that different frequencies of tone production relate to the activity of different vents. In this case, the switching on and off of different

tremor frequencies at ~0.6 Hz and ~0.8 Hz (Figure 3a) may simply correspond to intermittent activity at separate vents. However, between 0300 and 0600 UTC Julian day 111 2007 (Figure 3a), the lower frequency peak of ~0.6 Hz appears to diverge progressively from the peak at ~0.8 Hz at a bifurcation in the frequency domain. This property suggests that both frequency peaks are related to a single mechanism such as sound production by evolving flow conditions at a single vent.

[33] The seismic tremor data at KIPU have a complicated spectrum (Figure 3b), with some sharp peaks between ~0.6 and 0.9 Hz in common with the infrasound data, but other peaks and broadband noise distributed throughout the 1–10 Hz band. In the framework of our discussion, the common peaks between ~0.6 and 0.9 Hz suggest that the proposed hole-tone or whistler nozzle infrasound source process is also a seismic source. This could be achieved by acoustic energy coupling into the solid boundaries of the resonant cavity of length L in the schematic Figure 3c. It may also be achieved by air-ground coupling outside of the source region. The other peaks and broadband noise in the 1–10 Hz band of the seismic data may indicate modification of the wavefield from the same tremor source processes responsible for the infrasonic signal by additional source or path resonances [*Goldstein and Chouet*, 1994; *Chouet*, 1996], or it may indicate that additional deeper seismic sources are also present that are isolated from the atmosphere.

[34] Finally, we comment that fully turbulent volcanic flows can generate powerful infrasound, which may be analogous to audible jet noise produced by smaller-scale turbulent jet flows [*Matoza et al.*, 2009]. However, the mechanism discussed here refers to lower speed and therefore lower Reynolds number flows. In fact, a laminar jet can produce self-sustained oscillations when impinging on a solid object [*Rockwell and Naudascher*, 1979; *Chanaud and Powell*, 1965; *Howe*, 1998], and it is typically observed that laminar flows produce more intense and better defined flow-induced spectral peaks [*Chanaud and Powell*, 1965; *Howe*, 1998]. When the flows become more turbulent, the tones generated by impingement feedback become less defined, and can be overwhelmed by the broadband noise from turbulence (although supersonic jet flows can exhibit additional spectral peaks referred to as jet screech [*Tam*, 1995]). In this sense, the sharply peaked harmonic tremor observed at Pu`u `Ō`ō, and at other volcanoes [*Garcés et al.*, 2008], may be related to the more energetic and broadband tremor associated with more vigorous Vulcanian and Plinian volcanic eruptions [*Matoza et al.*, 2009]. Both may result from jet aeroacoustic processes, with the Reynolds number of the flow being a key parameter determining whether harmonic or more broadband (jet noise-like) infrasonic tremor is produced. In this framework, the geometry of the volcanic vent and nozzle, and the resonant modes of the upper conduit section would be other critical factors controlling the spectral nature of infrasonic tremor resulting from degassing at various flow speeds.

6. Signals From the Lava Tube System

[35] At intermittent times throughout the field deployment, audible noises resembling jet noise, chugging [*Johnson and Lees*, 2000], and more resonant harmonic tremor could be heard for up to several hours at a time and originated from south of the main crater complex area. At most of these times, little or no change in the KIPU infrasound data was observed. However, during at least one time (1200 to 1700 UTC Julian day 112 2007), very intense audible chugging and jet noise sounds were heard at the same time that PMCC processing results show additional infrasonic energy in the 5–10 Hz band arriving from a location on the south flank (Figure 8a). However, the infrasound arrays with aperture of ~100 m have an array response which results in spatial aliasing above frequencies of ~5 Hz. Thus, array processing in the 5–10 Hz band for KIPU results in numerous spurious signals and the results must be interpreted with caution. Nevertheless, PMCC processing can perform well on ground-truth signals with frequencies extending well above the optimal array response (see Figure 9a of *Matoza et al.* [2007] in which a similar array geometry and aperture were used). In addition, we applied strict postprocessing parsing of the 5–10 Hz PMCC results to remove the spurious azimuth detections (Figure 8a), and correlated the PMCC results with changes in the waveform envelope during these time periods. During the times in which intense audible sounds were heard, PMCC detections in the 5–10 Hz band shift to the south and point to a location along the lava tube system. This does not indicate cessation of the crater complex source, which is seen to be continuous in the 0.5–5 Hz band (Figure 2), but suggests instead that the source to the south dominated in the 5–10 Hz band.

[36] Infrared imaging from the KIPU array site revealed an incandescent source in the approximate direction from which audible sound and infrasound originated (Figure 8b). Subsequent investigation of this area revealed a new skylight opening in the lava tube system which had not been previously documented (Figure 8c). The vent was surrounded by spatter indicative of increased degassing/spattering activity (Figure 8c). These observations indicate that vents in the extended lava tube system can be sources of infrasonic tremor in addition to the vents in the crater complex area and suggest that infrasound arrays could help to monitor the lava tube system for new vent openings. The evidence for degassing activity is consistent with the acoustic source process outlined in section 5.3. The smaller size of this vent in comparison to the larger vents in the crater complex area may explain why these signals had higher dominant frequencies than the signals from the crater complex area.

[37] The intermittent acoustic and degassing activity of the vent shown in Figure 8c has implications for skylight formation, lava tube dynamics, and acoustic source dynamics in the lava tube system. On the night of Julian day 115 after the photograph shown in Figure 8c was taken, the audible jet noise sounds were heard again, indicating that vigorous (turbulent) degassing had reinitiated at the vent. On the following day (Julian day 116) we returned to the skylight, and found that the skylight opening had been eroded and heavily spattered, and that the vent area features were unrecognizable. Lava in this downstream section of the lava tube system is usually considered essentially degassed of volatiles other than water [*Edmonds and Gerlach*, 2007], yet the jetting activity and erosion/dynamics of the vent region suggest vigorous degassing activity from an abundant volatile source. It is possible that a pocket of gas intermittently managed to make it downstream to this location, where it

was then released causing erosion of the skylight and the jetting activity. In another scenario, solid pieces of the lava tube may have intermittently collapsed into the lava, triggering degassing. Alternatively, heavy rainfall during the experiment may have provided meteoric input to the system [*Keszthelyi*, 1995], providing an intermittent volatile flux. A sudden change in the lava tube geometry such as a step down in elevation (lava fall), or a constriction in the tube diameter, might be responsible for disrupting the flow and releasing the gas at this specific location. Some of the questions pertaining to lava tube dynamics [*Greeley*, 1987; *Helz et al.*, 2003] and skylight formation could be addressed with future focused acoustic studies.

7. Conclusions

[38] The temporary deployment of a broadband infrasound array ~2.4 km from Pu`u `Ō`ō, in conjunction with a semipermanent array at ~12.5 km range, enabled clarification of the propagation effects on the infrasonic tremor wavefield at Kilauea Volcano. The deployment of the array closer to Pu`u `Ō`ō also enabled recordings of the tremor signal that had higher signal-to-noise ratios and were relatively free from propagation effects. The persistent infrasonic tremor source contains at least two components (1) a broadband component concentrated between 0.5 and 15 Hz, and (2) more sharply peaked tones in the 0.6–0.9 Hz band that exhibit complex temporal evolution. We speculate that (1) may be generated primarily by bubble cloud oscillations in a roiling lava body beneath the crater complex, while (2) may result from interaction of the escaping stream of gas with the vent and near-surface cavities in a process similar to the hole tone or whistler nozzle phenomenon. However, further work is required to assess the theoretical source power and radiation properties of these processes. Additional infrasonic and audible sounds originating from the south flank coincided with increased degassing activity at a relatively new lava tube skylight, suggesting that acoustic studies may aid in monitoring and understanding flow dynamics in the lava tube system.

[39] **Acknowledgments.** KIPU was deployed with helicopter field support from HVO. We are very grateful to Frank Trusdell for hosting the MENE array in his backyard and to Tim Orr for advice on accessible vents. James Robertson and Emily Crawford helped with the field deployment and KIPU array site survey. THST wind tower data were provided by Thomas Giambelluca, Guangxia Cao, and Kate Brauman. Bernard Chouet provided some insightful comments on an early version of the manuscript. We thank two anonymous reviewers and an associate editor. This work was funded by NSF grant EAR-0609669.

References

Buckingham, M. J., and M. A. Garcés (1996), Canonical model of volcano acoustics, *J. Geophys. Res.*, *101*(B4), 8129–8151, doi:10.1029/95JB01680.

Busse, F. H., P. A. Monkewitz, and M. Hellweg (2005), Are harmonic tremors self-excited thermoacoustic oscillations?, *Earth Planet. Sci. Lett.*, *240*, 302–306, doi:10.1016/j.epsl.2005.09.046.

Cansi, Y. (1995), An automatic seismic event processing for detection and location: The P.M.C.C. method, *Geophys. Res. Lett.*, *22*(9), 1021–1024, doi:10.1029/95GL00468.

Chanaud, R. C., and A. Powell (1965), Some experiments concerning the hole and ring tone, *J. Acoust. Soc. Am.*, *37*(5), 902–911, doi:10.1121/1.1909476.

Chouet, B., and H. R. Shaw (1991), Fractal properties of tremor and gas piston events observed at Kilauea Volcano, Hawaii, *J. Geophys. Res.*, *96*(B6), 10,177–10,189, doi:10.1029/91JB00772.

Chouet, B. A. (1996), New methods and future trends in seismological volcano monitoring, in *Monitoring and Mitigation of Volcano Hazards*, edited by R. Scarpa and R. Tilling, pp. 23–97, Springer, New York.

Commander, K. W., and A. Prosperetti (1989), Linear pressure waves in bubbly liquids: Comparison between theory and experiments, *J. Acoust. Soc. Am.*, *85*(2), 732–746, doi:10.1121/1.397599.

DeFatta, D. J., J. G. Lucas, and W. S. Hodgkiss (1988), *Digital Signal Processing: A System Design Approach*, John Wiley, New York.

Delprat, N. (2006), Rossiter's formula: A simple spectral model for a complex amplitude modulation process?, *Phys. Fluids*, *18*, 071703, doi:10.1063/1.2219767.

Edmonds, M., and T. M. Gerlach (2007), Vapor segregation and loss in basaltic melts, *Geology*, *35*, 751–754, doi:10.1130/G23464A.1.

Fee, D., and M. Garcés (2007), Infrasonic tremor in the diffraction zone, *Geophys. Res. Lett.*, *34*, L16826, doi:10.1029/2007GL030616.

Fee, D., M. Garces, M. Patrick, B. A. Chouet, P. Dawson, and D. Swanson (2010), Infrasonic harmonic tremor and degassing bursts from Halema`uma`u Crater, Kilauea Volcano, Hawaii, *J. Geophys. Res.*, doi:10.1029/2010JB007642, in press.

Ferrazzini, V., K. Aki, and B. Chouet (1991), Characteristics of seismic waves composing Hawaiian volcanic tremor and gas-piston events observed by a near source array, *J. Geophys. Res.*, *96*(B4), 6199–6209, doi:10.1029/90JB02781.

Fletcher, N. H. (1999), The nonlinear physics of musical instruments, *Rep. Prog. Phys.*, *62*, 723–764, doi:10.1088/0034-4885/62/5/202.

Fletcher, N. H., and T. D. Rossing (2008), *The Physics of Musical Instruments*, 2nd ed., Springer, New York.

Garcés, M. A. (1997), On the volcanic waveguide, *J. Geophys. Res.*, *102*(B10), 22,547–22,564, doi:10.1029/97JB01799.

Garcés, M. A. (2000), Theory of acoustic propagation in a multiphase stratified liquid flowing within an elastic-walled conduit of varying cross-sectional area, *J. Volcanol. Geotherm. Res.*, *101*, 1–17, doi:10.1016/S0377-0273(00)00155-4.

Garcés, M. A., and S. R. McNutt (1997), Theory of the airborne sound field generated in a resonant magma conduit, *J. Volcanol. Geotherm. Res.*, *78*, 155–178, doi:10.1016/S0377-0273(97)00018-8.

Garcés, M. A., M. T. Hagerty, and S. Y. Schwartz (1998), Magma acoustics and time-varying melt properties at Arenal Volcano, Costa Rica, *Geophys. Res. Lett.*, *25*(13), 2293–2296, doi:10.1029/98GL01511.

Garcés, M., A. Harris, C. Hetzer, J. Johnson, S. Rowland, E. Marchetti, and P. Okubo (2003), Infrasonic tremor observed at Kīlauea Volcano, Hawai'i, *Geophys. Res. Lett.*, *30*(20), 2023, doi:10.1029/2003GL018038.

Garcés, M. A., D. Fee, D. McCormack, R. Servranckx, H. Bass, C. Hetzer, M. Hedlin, R. Matoza, and H. Yepes (2008), Prototype ASHE volcano monitoring system captures the acoustic fingerprint of stratospheric ash injection, *Eos Trans. AGU*, *89*(40), 377.

Gerst, A., M. Hort, P. R. Kyle, and M. Voge (2008), 4D velocity of Strombolian eruptions and man-made explosions derived from multiple Doppler radar instruments, *J. Volcanol. Geotherm. Res.*, *177*(3), 648–660, doi:10.1016/j.jvolgeores.2008.05.022.

Godin, O. A. (2006), Anomalous transparency of water-air interface for low-frequency sound, *Phys. Rev. Lett.*, *97*, 164301, doi:10.1103/PhysRevLett.97.164301.

Godin, O. A. (2007), Transmission of low-frequency sound through the water-to-air interface, *Acoust. Phys.*, *53*(3), 305–312, doi:10.1134/S1063771007030074.

Goldstein, P., and B. Chouet (1994), Array measurements and modeling of sources of shallow volcanic tremor at Kilauea Volcano, Hawaii, *J. Geophys. Res.*, *99*(B2), 2637–2652, doi:10.1029/93JB02639.

Greeley, R. (1987), The role of lava tubes in Hawaiian volcanoes, in *Volcanism in Hawaii*, edited by R. W. Decker, T. L. Wright, and P. H. Stauffer, *U.S. Geol. Surv. Prof. Pap.*, *1350*, 1589–1602.

Hahn, T. R., T. K. Berger, and M. J. Buckingham (2003), Acoustic resonances in the bubble plume formed by a plunging water jet, *Proc. R. Soc. London A*, *459*, 1751–1782, doi:10.1098/rspa.2002.1063.

Heliker, C., and T. N. Mattox (2003), The first two decades of the Pu`u `Ō`ō-Kūpaianaha eruption: Chronology and selected bibliography, in *The Pu`u `O`o-Kupaianaha Eruption of Kilauea Volcano, Hawai`i: The First 20 Years*, edited by C. Heliker, D. Swanson, and T. Takahashi, *U.S. Geol. Surv. Prof. Pap.*, *1676*, 1–28.

Helz, R. T., C. Heliker, K. Hon, and M. Mangan (2003), Thermal efficiency of lava tubes in the Pu`u `Ō`ō-Kūpaianaha eruption, in *The Pu`u `O`o-Kupaianaha Eruption of Kilauea Volcano, Hawai`i: The First 20 Years*, edited by C. Heliker, D. Swanson, and T. Takahashi, *U.S. Geol. Surv. Prof. Pap.*, *1676*, 105–120.

Hirschberg, A., J. C. Bruggeman, A. P. J. Wijnands, and N. Smits (1989), The "whistler nozzle" and horn as aeroacoustic sound sources in pipe systems, *Acustica*, *68*, 157–160.

Howe, M. S. (1998), *Acoustics of Fluid-Structure Interactions*, Cambridge Univ. Press, Cambridge, U. K., doi:10.1017/CBO9780511662898

Hussain, A. K. M. F., and M. A. Z. Hasan (1983), The "whistler-nozzle" phenomenon, *J. Fluid Mech.*, *134*, 431–458, doi:10.1017/S0022112083003420.

Ichihara, M., and M. Kameda (2004), Propagation of acoustic waves in a visco-elastic two-phase system: Influences of the liquid viscosity and the internal diffusion, *J. Volcanol. Geotherm. Res.*, *137*(1–3), 73–91, doi:10.1016/j.jvolgeores.2004.05.001.

Johnson, J., R. Aster, K. R. Jones, P. Kyle, and B. McIntosh (2008), Acoustic source characterization of impulsive Strombolian eruptions from the Mount Erebus lava lake, *J. Volcanol. Geotherm. Res.*, *177*(3), 673–686, doi:10.1016/j.jvolgeores.2008.06.028.

Johnson, J. B., and J. M. Lees (2000), Plugs and chugs—Seismic and acoustic observations of degassing explosions at Karymsky, Russia and Sangay, Ecuador, *J. Volcanol. Geotherm. Res.*, *101*, 67–82, doi:10.1016/S0377-0273(00)00164-5.

Julian, B. R. (1994), Volcanic tremor: Nonlinear excitation by fluid flow, *J. Geophys. Res.*, *99*(B6), 11,859–11,877, doi:10.1029/93JB03129.

Keszthelyi, L. (1995), A preliminary thermal budget for lava tubes on the Earth and planets, *J. Geophys. Res.*, *100*(B10), 20,411–20,420, doi:10.1029/95JB01965.

Langthjem, M. A., and M. Nakano (2005), A numerical simulation of the hole-tone feedback cycle based on an axisymmetric discrete vortex method and Curle's equation, *J. Sound Vibrat.*, *288*, 133–176, doi:10.1016/j.jsv.2004.12.023.

Leighton, T. G. (1994), *The Acoustic Bubble*, Academic, New York.

Lu, N. Q., A. Prosperetti, and S. W. Yoon (1990), Underwater noise emissions from bubble clouds, *IEEE J. Oceanic Eng.*, *15*(4), 275–281, doi:10.1109/48.103521.

Malone, J., M. Debiasi, J. Little, and M. Samimy (2009), Analysis of the spectral relationships of cavity tones in subsonic resonant cavity flows, *Phys. Fluids*, *21*, 055103, doi:10.1063/1.3139270.

Marchetti, E., and A. J. L. Harris (2008), Trends in activity at Pu`u O`o during 2001–2003: Insights from the continuous thermal record, *Geol. Soc. Spec. Publ.*, *307*, 85–101, doi:10.1144/SP307.6.

Marchetti, E., M. Ichihara, and M. Ripepe (2004), Propagation of acoustic waves in a viscoelastic two-phase system: Influence of gas bubble concentration, *J. Volcanol. Geotherm. Res.*, *137*(1–3), 93–108, doi:10.1016/j.jvolgeores.2004.05.002.

Matoza, R. S., M. A. H. Hedlin, and M. A. Garcés (2007), An infrasound array study of Mount St. Helens, *J. Volcanol. Geotherm. Res.*, *160*, 249–262, doi:10.1016/j.jvolgeores.2006.10.006.

Matoza, R. S., D. Fee, M. A. Garcés, J. M. Seiner, P. A. Ramon, and M. A. H. Hedlin (2009), Infrasonic jet noise from volcanic eruptions, *Geophys. Res. Lett.*, *36*, L08303, doi:10.1029/2008GL036486.

Nyborg, W. L., M. D. Burkhard, and H. K. Schilling (1952), Acoustical characteristics of jet-edge and jet-edge-resonator systems, *J. Acoust. Soc. Am.*, *24*(3), 293–304, doi:10.1121/1.1906894.

Park, J., M. Garcés, D. Fee, and G. Pawlak (2008), Collective bubble oscillations as a component of surf infrasound, *J. Acoust. Soc. Am.*, *123*(5), 2506–2512, doi:10.1121/1.2885743.

Perret, F. A. (1950), Volcanological observations, *Carnegie Inst. Washington Publ.*, *549*, 162 pp.

Poland, M., A. Miklius, T. Orr, J. Sutton, C. Thornber, and D. Wilson (2008), New episodes of volcanism at Kilauea Volcano, Hawaii, *Eos Trans. AGU*, *89*(5), 37, doi:10.1029/2008EO050001.

Raspet, R., J. Webster, and K. Dillion (2006), Framework for wind noise studies, *J. Acoust. Soc. Am.*, *119*(2), 834–843, doi:10.1121/1.2146113.

Raspet, R., J. Yu, and J. Webster (2008), Low frequency wind noise contributions in measurement microphones, *J. Acoust. Soc. Am.*, *123*(3), 1260–1269, doi:10.1121/1.2832329.

Rayleigh, J. W. S. (1976), *The Theory of Sound*, vol. 2, 2nd ed., Dover, Mineola, N. Y.

Richards, A. F. (1963), Volcanic sounds: Investigation and analysis, *J. Geophys. Res.*, *68*(3), 919–928, doi:10.1029/JZ068i003p00919.

Ripepe, M., E. Marchetti, and G. Ulivieri (2007), Infrasonic monitoring at Stromboli volcano during the 2003 effusive eruption: Insights on the explosive and degassing process of an open conduit system, *J. Geophys. Res.*, *112*, B09207, doi:10.1029/2006JB004613.

Rockwell, D., and E. Naudascher (1978), Review—Self-sustaining oscillations of flow past cavities, *ASME Trans. J. Fluids Eng.*, *100*, 152–165, doi:10.1115/1.3448624.

Rockwell, D., and E. Naudascher (1979), Self-sustained oscillations of impinging free shear layers, *Annu. Rev. Fluid Mech.*, *11*, 67–94, doi:10.1146/annurev.fl.11.010179.000435.

Rossiter, J. E. (1964), Wind-tunnel experiments on the flow over rectangular cavities at subsonic and transonic speeds, *Rep. Memo. 3438*, Minist. of Aviat, London.

Shaw, H. R. (1972), Viscosities of magmatic silicate liquids: An empirical method of prediction, *Am. J. Sci.*, *272*, 870–893, doi:10.2475/ajs.272.9.870.

Swift, G. W. (2007), Thermoacoustics, in *Springer Handbook of Acoustics*, edited by T. Rossing, pp. 239–255, Springer, New York, doi:10.1007/978-0-387-30425-0_7.

Tam, C. K. W. (1995), Supersonic jet noise, *Annu. Rev. Fluid Mech.*, *27*, 17–43, doi:10.1146/annurev.fl.27.010195.000313.

van Wijngaarden, L. (1972), One-dimensional flow of liquids containing small gas bubbles, *Annu. Rev. Fluid Mech.*, *4*, 369–396, doi:10.1146/annurev.fl.04.010172.002101.

Vergniolle, S., and G. Brandeis (1996), Strombolian explosions: 1. A large bubble breaking at the surface of a lava column as a source of sound, *J. Geophys. Res.*, *101*(B9), 20,433–20,447, doi:10.1029/96JB01178.

Webb, S. (1997), Silicate melts: Relaxation, rheology, and the glass transition, *Rev. Geophys.*, *35*(2), 191–218, doi:10.1029/96RG03263.

Wilson, P. S., and R. A. Roy (2008), An audible demonstration of the speed of sound in bubbly liquids, *Am. J. Phys.*, *76*(10), 975–981, doi:10.1119/1.2907773.

Wilson, T. A., G. S. Beavers, M. A. DeCoster, D. K. Holger, and M. D. Regenfuss (1971), Experiments on the fluid mechanics of whistling, *J. Acoust. Soc. Am.*, *50*, 366–372, doi:10.1121/1.1912641.

Wood, A. B. (1964), *A Textbook of Sound*, 3rd ed., G. Bell, London.

Woulff, G., and T. R. McGetchin (1976), Acoustic noise from volcanoes: Theory and experiment, *Geophys. J. R. Astron. Soc.*, *45*, 601–616.

Yoon, S. W., L. A. Crum, A. Prosperetti, and N. Q. Lu (1991), An investigation of the collective oscillations of a bubble cloud, *J. Acoust. Soc. Am.*, *89*(2), 700–706, doi:10.1121/1.1894629.

D. Fee, Wilson Infrasound Observatories, Geophysical Institute, University of Alaska Fairbanks, 903 Koyukuk Dr., Fairbanks, AK 99775-7320, USA. (dfee@gi.alaska.edu)

M. A. Garcés, Infrasound Laboratory, University of Hawaii at Manoa, 73-4460 Queen Kaahumanu Hwy., 119, Kailua-Kona, HI 96740, USA. (milton@isla.hawaii.edu)

R. S. Matoza, CEA/DAM/DIF, F-91297 Arpajon, France. (robin.matoza@cea.fr)